




EX LIBRIS
UNIVERSITATIS
ALBERTENSIS

The Bruce Peel
Special Collections
Library



Digitized by the Internet Archive
in 2025 with funding from
University of Alberta Library

<https://archive.org/details/0162015157900>

University of Alberta

Library release form

Name of Author: Muhammad Riaz

Title of Thesis: Robust Observer Design using H-infinity Approach

Degree: Master of Science

Year this Degree Granted: 2001

Permission is hereby granted to the University of Alberta Library to reproduce single copies of this thesis and to lend or sell such copies for private, scholarly or scientific research purposes only.

The author reserves all other publication and other rights in association with the copy right in the thesis, and except as herein before provided, neither the thesis nor any substantial portion thereof may be printed or otherwise reproduced in any material form whatever without the authors prior written permission.

University of Alberta

**ROBUST OBSERVER DESIGN USING H-INFINITY
APPROACH**

by

Muhammad Riaz



A thesis submitted to the Faculty of Graduate Studies and Research in partial fulfillment of the requirements for the degree of **Master of Science**

in

Control Systems

Department of Electrical and Computer Engineering

Edmonton, Alberta

Fall 2001

University of Alberta

Faculty of Graduate Studies and Research

The undersigned certify that they have read, and recommend to the Faculty of Graduate Studies and Research for acceptance, a thesis entitled **Robust Observer Design using H-infinity Approach** submitted by **Muhammad Riaz** in partial fulfillment of the requirements for the degree of **Master of Science** in Control Systems.

To

my parents and my teachers

for their support in crucial moments of my life

Abstract

This report presents the development and design of the Observer for state estimation in the presence of plant-model mismatch. A new observer structure is introduced which is based on the robust control problem in the H-infinity framework. The estimation problem is reduced to H-infinity control problem. The strength and weaknesses of proposed design methodology are discussed. This design approach is applied to an experimentally verified simulation model of Utility Boiler at **Syncrude** power plant, Mildred Lake, Alberta. The boiler selected exhibits non-linearities, time delays and non-minimum phase behavior. The design shows the limitation imposed on estimation problem due to time delays and non- minimum phase. The report also demonstrates the trade-off between the speed of the observer and the estimation error. To deal with the non-linear behavior of the utility boiler, the approach of linearization over selected operating range is considered. Observer for each operating range is designed. The resultant observer bank is tested over the entire operating range and conclusions are drawn for the real-time applications.

Acknowledgement

I would like to thank those people who made this research not only possible, but also worthwhile and enjoyable. A special note of appreciation to my supervisor Dr. Horacio J. Marquez whose enthusiasm for and insight into the subject provided a constant source of encouragement. Special thanks are due to my co-supervisor Professor Tongwen Chen for his financial support at the early stage of the program and his useful and constructive suggestions during all these two years.

This research was partially supported by Syncrude Canada Ltd. I would like to thank Mr. Kent Gooden of Syncrude Canada Ltd. for initiating the collaborative research and development grant and his insight into real plant issues. I would like to express my deepest sense of gratitude to Dr. Ray Rink for his valuable suggestions specifically regarding modeling and simulation part of this work. In addition thanks are due to Dr. Wen Tan and Bushan Gopaloni for sharing their knowledge and experience.

Finally I would like to thank my brothers, sisters and friends for their co-operation & understanding, my wife for her patience, and my parents for their prayers that made it possible to undertake and accomplish this work.

Contents

1	Introduction	1
1.1	Dynamic Systems and the Concept of State	2
1.2	Introduction to Observer	5
1.3	The Problem and Approach to Solution	9
1.4	Literature Survey	13
1.5	Contribution	14
1.6	Introduction to Syncrude Power Plant	15
1.6.1	Utility Boiler	16
1.7	Thesis Organization	19
2	Proposed Observer Scheme	21
2.1	Input to State Uncertainty Approach	22
2.2	An Input-Output Observer	25
2.3	Observer Stability	31
2.4	Observer Properties	36
2.5	Comments	38
3	Model Identification	40
3.1	Objective and Methodology	41
3.2	Numerical Sub-Space State Space Identification	42
3.3	Selection of Input and Output Parameters	43
3.4	Physical Interpretation of States	45
3.5	Input Signal Design	47
3.6	Steady State Operating Points	49
3.7	Utility Boiler Models	50

4	Observer Design	54
4.1	H_∞ Optimal Control	54
4.2	H_∞ Loop Shaping Design	58
4.3	Controller Model Order Reduction	61
4.4	Observer Design	62
4.4.1	Observer Design for HOP	63
4.4.2	Observer Design for MOP	77
4.4.3	Observer Design for LOP	82
4.4.4	Comments	87
5	Observer Scheduling	88
5.1	Gain Scheduling	88
5.2	Observer Scheduling	90
5.3	Simulation Results	91
6	Conclusion	103
	Bibliography	107
	Appendix A	109
	Appendix B	110

List of Figures

1.1	Observer	6
1.2	Luenberger Observer	8
1.3	Natural Re-circulation Water Tube Boiler	18
2.1	Relationship of System P with F and C	23
2.2	Uncertainty Representation	24
2.3	Input Output Observer	26
2.4	Interconnected System	29
2.5	The System S1	32
2.6	The System S2	35
3.1	Random Binary Signal Applied as Input	49
3.2	Drum pressure Response to Step change in Steam Load (LOP)	51
3.3	Drum pressure Response to Step change in Steam Load (MOP)	52
3.4	Drum pressure Response to Step change in Steam Load (HOP)	53
4.1	Standard \mathbf{H}_∞ Formulation	55
4.2	General \mathbf{H}_∞ Formulation with Weightings	57
4.3	Shaped Plant for Case-I	65
4.4	Singular Value Plot of Sensitivity Function (HOP: Case-I)	67
4.5	Output Step Response using $\mathbf{G}1_c$ (HOP: Case-I)	67

4.6	Shaped Plant P_s (HOP: Case-II)	69
4.7	Singular Value Plot of Sensitivity Function (HOP: Case-II)	71
4.8	Output Step Response using G1 (HOP: Case-II)	71
4.9	Singular Value Plot of $ S $ with G1_l , G1_r and G1_h	73
4.10	Step Response using G1 , G1_r and G1_h	73
4.11	Estimated vs. Actual Furnace Gas Temperature (HOP)	75
4.12	Estimated vs. Actual Super Heater Gas Temperature (HOP)	76
4.13	Estimated vs. Actual Economizer Gas Temperature (HOP)	76
4.14	Shaped Plant P_s (MOP)	78
4.15	Singular Value Plot of $ S $ using G2 (MOP)	79
4.16	Output Response using G2 and G2_h (MOP)	79
4.17	Singular Value Plot of $ S $ with G2 and G2_h (MOP)	80
4.18	Estimated vs. Actual Furnace Gas Temperature (MOP)	80
4.19	Estimated vs. Actual Super Heater Gas Temperature (MOP)	81
4.20	Estimated vs. Actual Economizer Gas Temperature (MOP)	81
4.21	Shaped Plant P_s (LOP)	83
4.22	Singular Value Plot of $ S $ using G3 (LOP)	83
4.23	Output Step Response using G3 (LOP)	84
4.24	Singular Value Plot of $ S $ with G3 and G3_h (LOP)	84
4.25	Estimated vs. Actual Furnace Gas Temperature (LOP)	85
4.26	Estimated vs. Actual Super Heater Gas Temperature (LOP)	85
4.27	Estimated vs. Actual Economizer Gas Temperature (LOP)	86

5.1	Observer Scheduling Implementation Layout	92
5.2	Multi-step Steam Load Change	93
5.3	Furnace Gas Temperature (Plant vs. Observer 1)	95
5.4	Furnace Gas Temperature (Plant vs. Observer 2)	95
5.5	Furnace Gas Temperature (Plant vs. Observer 3)	96
5.6	Super Heater Gas Temperature (Plant vs. Observer 1)	97
5.7	Super Heater Gas Temperature (Plant vs. Observer 2)	97
5.8	Super Heater Gas Temperature (Plant vs. Observer 3)	98
5.9	Economizer Gas Temperature (Plant vs. Observer 1)	98
5.10	Economizer Gas Temperature (Plant vs. Observer 2)	99
5.11	Economizer Gas Temperature (Plant vs. Observer 3)	99
5.12	Furnace Gas Temperature (Plant vs. Observer Bank)	101
5.13	Super Heater Gas Temperature (Plant vs. Observer Bank)	101
5.14	Economizer Gas Temperature (Plant vs. Observer Bank)	102

Chapter 1

Introduction

In this chapter, the concept of state estimation and state observer is introduced and the problem to be studied in this thesis is elaborated. At the end of the chapter, an overview of Syncrude power plant is provided followed by a discussion on the physics of utility boiler to which further developments will be applied.

Improved process monitoring and control is the key to efficiently operate co-generation plant while ensuring reliability of steam supply and electric power at the same time. Stability of complex interactive systems is always an issue and cannot be achieved without effective control. Better control and monitoring can be achieved by measuring enough process data and processing that data using established control algorithms. Although a fair amount of process measurement data is usually available, it is not possible to measure every quantity and transmit it to the control center. This limitation can be attributed to high cost of measurement devices and field wiring and low available bandwidth for transmission. The reasonable approach would be to estimate that data, which is not available as sensor output but is required for applications like state feedback or fault detection. The best candidate for estimation would be *state* variables of a dynamic system.

1.1 Dynamic Systems and the Concept of State

In most general meaning the term *system* refers to some physical entity on which some action is performed by means of input u . The system reacts to this input and produces an output y .

A *dynamic system* is a system whose phenomena occur over time. One often says that a system *evolves over time*.

Consider a system with single input $u(t)$ and single output $y(t)$, and assume that the system does not contain any independent sources and is at rest with no internal energy, before the signal is applied. The input-output relationship is often indicated symbolically by

$$y(t) = L u(t)$$

where L is an operator that characterizes the system. It may be a function of u , y and t ; it may include operations such as differentiation and integration; and it may be given in probabilistic language. The above equation is not more than a short way of saying that there is some cause and effect relationship between $u(t)$ and $y(t)$.

A system is deterministic if for each input $u(t)$ there is a unique output $y(t)$. In non-deterministic or probabilistic system, there may be several possible outputs, each with a certain degree of probability of occurrence, for a given input. Input to a system may also be given either as known functions or as random functions. If a random signal is input to a deterministic system the output is not deterministic.

State of a system is the smallest set of variables such that the knowledge of these variables at $t = t_0$ (initial condition) together with the inputs completely determines the behavior of the system for any time $t > t_0$.

For an example of the state of a system, consider the solution of a linear constant-coefficient differential equation for $t \geq t_o$. Once the form of a complete solution is obtained in terms of arbitrary constants, these constants can then be determined by the fact that the system must satisfy boundary conditions at time t_o . No other information is required. The boundary conditions can then be termed as the state of the system at time t_o . Heuristically, the state of a system separates the future from the past, so that state contains all the relevant information concerning the past history of the system required to determine the response for any input.

The idea of state is a fundamental concept and therefore cannot be defined any more than, for example the word “set” can be defined in mathematics. The most that can be done is to state the properties required of a system whose behavior involves the notion of state.

Given a dynamic system, the modeling problem is to some how correlate the inputs (causes) with outputs (effects). The output at time t cannot be determined in general by the value assumed by the input quantity at the same point in time. Rather the output is the result of the entire history of the system. An effort of abstraction is therefore required, which leads to postulating a new quantity, called the *state*, which summarizes the information about the past and present of the system. The value $x(t)$ taken by the state at time t must be sufficient to determine the output at the same point in time. Also, knowledge of both $x(t_1)$ and $u(t_1, t_2)$, that is, of the state at time t_1 and the input over interval $t_1 \leq t < t_2$, must allow computing the state (hence the output) at time t_2 . Thus in a dynamic system the input affects the state, and the output is a function of the state.

The important terms associated with state concept are *state variables* and *state space* and it would be good to define them in simple words. If n state variables are necessary to determine the behavior of a given system, the variables can be considered as n components of a vector called *state vector*. The n dimensional state variables are elements of n dimensional space called *state space*.

In case of continuous time systems, one can show that there exists a function 'f' such that the state $x(t)$ of the system satisfies the differential equation

$$\dot{x}(t) = f[x(t), u(t), t]$$

where the dot denote differentiation with respect to time and the relation from state to output is

$$y(t) = h[x(t), t]$$

Specifying the initial state x_0 completes the definition of continuous time dynamic system.

For a linear time invariant multi-input multi-output system, the above state-space representation takes on the form

$$\dot{\mathbf{x}} = \mathbf{Ax} + \mathbf{Bu}$$

$$\mathbf{y} = \mathbf{Cx}$$

where for p inputs, m outputs and n states, \mathbf{A} is $n \times n$ matrix, \mathbf{B} is $n \times m$ and \mathbf{C} is $p \times n$ matrix.

1.2 Introduction to Observer

In most systems all components of the state vector are not directly available as output signals. Several approaches to the problem of unmeasured states can be considered. First it might be possible to add additional sensors to provide the measurements. This is generally the most expensive option. Second, some sort of ad hoc differentiation of measured states may provide an estimation of unmeasured states. This option may not give sufficiently accurate performance, especially in case of noisy data.

The third option is to use full knowledge of mathematical model of the system in a systematic way in an attempt to estimate or reconstruct the states. The resulting estimator algorithm is called an *observer*. Full state observers, some times called identity observers, produce estimates of all the state components even those variables, which are measured directly.

This redundancy can be removed with a *reduced state observer* that only estimates those states, which are not measured and uses raw measurement data for those that are measured directly. When measurements are noisy, the beneficial effects, which are provided by full state observer, may be more important than the elimination of redundancy.

The possible applications of an “Observer” or “State Estimation” can be:

1. State estimation for state feedback in process control.
2. Estimation of variables those are inaccessible to measurement for control or monitoring.
3. Prediction of unsafe process conditions for monitoring.
4. Sensor failure detection.

5. Estimation of process apparatus parameters, such as pump co-efficient, friction factors and valve characteristics.
6. State estimation of variables in environment likely to corrode or damage measuring instruments.

If the system is represented by state space realization of the form:

$$\dot{\mathbf{x}}(t) = \mathbf{A}(t)\mathbf{x}(t) + \mathbf{B}(t)\mathbf{u}(t)$$

$$\mathbf{y}(t) = \mathbf{C}(t)\mathbf{x}(t)$$

where $\mathbf{y}(t)$ and $\mathbf{u}(t)$ are the output and input of the plant respectively, then observer can be designed provided the state-space realization is observable. The estimated state vector $\hat{\mathbf{x}}(t)$ will be the output of the observer. Figure 1.1 shows general form of the observer and its connection with the plant output and input.

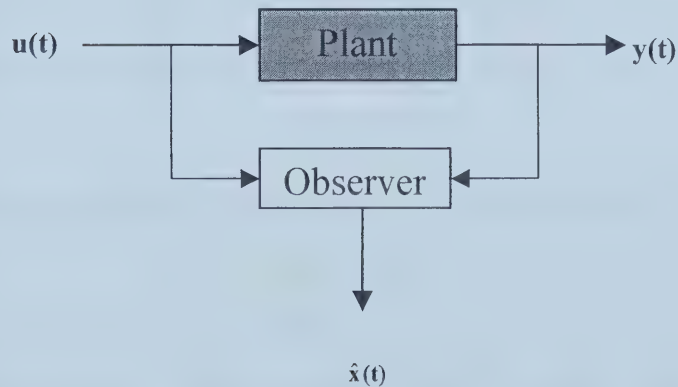


Figure 1.1: Observer

Generally in the solution of tracking and regulatory problems it is assumed that all the states are available. In most of the real systems this is not the case.

Most of the time for the system given below:

$$\begin{aligned}\dot{\mathbf{x}}(t) &= \mathbf{A}(t)\mathbf{x}(t) + \mathbf{B}(t)\mathbf{u}(t) \\ \mathbf{x}(t_0) &= \mathbf{x}_0\end{aligned}$$

Only some of the linear combinations of the state denoted by $\mathbf{y}(t)$, can be measured:

$$\mathbf{y}(t) = \mathbf{C}(t)\mathbf{x}(t)$$

The vector $\mathbf{y}(t)$ whose dimension usually is less than the state vector $\mathbf{x}(t)$, is referred to as the observed variable. The purpose of the observer is to reconstruct the state vector or finding approximations to the state vector from the observed variable.

The two types of observers commonly known are:

1. Luenberger Observer
2. Kalman Filter

The Kalman filter has the same structure as the Luenberger Observer but it also takes into consideration the noise factor. Here we will only discuss Luenberger Observer in detail.

Consider a system S defined by a minimal state space realization of the form

$$\begin{aligned}\dot{\mathbf{x}} &= \mathbf{Ax} + \mathbf{Bu} \\ \mathbf{y} &= \mathbf{Cx}\end{aligned}$$

Where \mathbf{u} is the input vector, \mathbf{y} the output vector, and \mathbf{x} is the state vector. \mathbf{A} , \mathbf{B} and \mathbf{C} are constant matrices representing the system dynamics. For simplicity we have assumed $\mathbf{D}=0$.

If we assume \mathbf{L} as the observer gain then observer is taken as a system defined by

$$\begin{aligned}\dot{\hat{\mathbf{x}}} &= \mathbf{A}\hat{\mathbf{x}} + \mathbf{B}\mathbf{u} + \mathbf{L}\mathbf{z} \\ \mathbf{y}_o &= \hat{\mathbf{x}}\end{aligned}$$

where $\hat{\mathbf{x}}$ is the estimated state and $\mathbf{e} = \mathbf{x} - \hat{\mathbf{x}}$ is the error between actual and estimated state, then

$$\dot{\mathbf{x}} - \dot{\hat{\mathbf{x}}} = \mathbf{A}(\mathbf{x} - \hat{\mathbf{x}}) - \mathbf{L}\mathbf{z}$$

$$\text{If we take } \mathbf{z} = \mathbf{y} - \hat{\mathbf{y}} = \mathbf{C}(\mathbf{x} - \hat{\mathbf{x}})$$

$$\text{Then } \dot{\mathbf{e}} = \dot{\mathbf{x}} - \dot{\hat{\mathbf{x}}} = (\mathbf{A} - \mathbf{L}\mathbf{C})(\mathbf{x} - \hat{\mathbf{x}})$$

The observer structure then becomes:

$$\dot{\hat{\mathbf{x}}} = \mathbf{A}\hat{\mathbf{x}} + \mathbf{B}\mathbf{u} + \mathbf{L}(\mathbf{y} - \hat{\mathbf{y}})$$

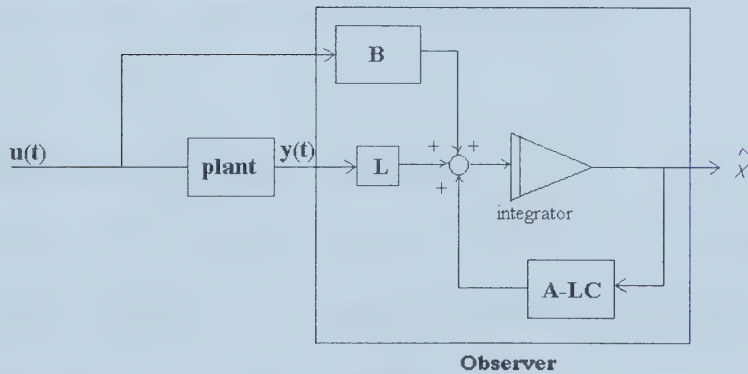


Figure 1.2: Luenberger Observer

If the eigenvalues of the matrix $(\mathbf{A} - \mathbf{L}\mathbf{C})$ lie in the left half of the complex plane, then the estimated state $\hat{\mathbf{x}}$ asymptotically converges to the true state \mathbf{x} . That is why this observer is some times called an asymptotic observer. The matrices \mathbf{A} and \mathbf{C} are the result of the plant, but matrix \mathbf{L} is to be chosen so that the state error \mathbf{e} dies out

rapidly. If the state space realization is completely observable then the observer can be designed to have arbitrary dynamics and the observer will then take the form as shown in figure 1.2.

Although the dynamics can be arbitrarily fast, there are some practical guidelines stated by [4] for choosing the eigenvalues of the observer.

- The eigenvalues of the observer should be more negative than that of the plant for rapid elimination of state error.
- Choosing the eigenvalues far in the left half plane makes the observer too sensitive to noise and this practice should be avoided.

Luenberger observer is a state estimator for the system, which may be corrupted by deterministic disturbances or noises. Kalman filter is the stochastic version of the observer, which incorporates stochastic noise with known statistics.

1.3 The Problem and Approach to Solution

To improve energy efficiency and reliability, better control and process monitoring is required at Syncrude power plant. State estimation is selected as the foundation block for the overall objective due to reasons mentioned below:

1. Most of the modern feedback control strategies need state feedback for better control of the plant. As in realistic problems all states are not always available, state estimation becomes an essential step in a controller design.
2. Some time operators need information about certain parameters that are difficult to measure. State estimation provides better alternative to collect that kind of information.

3. High level fault detection is generally achieved by applying observer based fault detectors. By using an observer as fault detector, the fault detection design problem is reduced to an estimation problem.
4. For prediction of unsafe process conditions, state measurement or estimation is required to generate alarms at process limits.

The purpose of the observer is to reconstruct the state vector or finding approximations to the state vector from the observed variable.

Observers are classified into two main categories by [10]:

- 1) Static Observers
- 2) Dynamic Observers

Kalman filter and Luenberger observer falls into the first category.

It is a matter of common knowledge that the Luenberger observer design is dual to state feedback, and the Kalman filter is dual to LQ design. The classical approach to state estimation consists of an unforced system with non-zero initial conditions. The error dynamics are stabilized to achieve asymptotic convergence by designing the observer gain. In case of Kalman filter, it is the minimum mean square linear estimator.

The observer theory has been developed long before the advanced control theories like H_∞ and LQG/LTR controller techniques. The observer design methods for the obvious reason could not take advantage of these mature theories. . For example, tracking and disturbance rejection problems could not be solved in an obvious way by the existing methods of optimal control [10]. The advanced linear control theories provide sound base for controller design, which can handle appropriately model

uncertainties and disturbance rejection. Robust stability and performance are also typical characteristics of them. In addition, output feedback controller design methods are more suitable for tracking and regulation problem.

Jong-Koo Park [10] and H.J.Marquez [5] gave the concept of dynamic state estimator. Both papers present the estimator problem as a linear feedback controller design problem. Following the footsteps of [10] and [5] we choose to design a dynamic state estimator. However, the virtues and shortcomings of the dynamic state estimator need to be further investigated. In this thesis we will concentrate our attention on the observer structure proposed in [5] and study the properties of this observer when applied to an industrial scale system. The system under consideration (described at the end of the chapter) has all the essential features encountered in real world applications and should constitute a good test for the proposed structure.

We propose a new observer structure based on robust control problem in an H_∞ framework. Thus the estimation problem is reduced to H_∞ control problem. H_∞ loop shaping technique is used to design the controller part of the observer. This method is easy to apply and is recommended by [11] for practical applications. It combines classical loop shaping with a powerful method of robust stabilization of feedback loop. For complex problems such as unstable plants with multiple crossover frequencies, it is difficult to come up with desired loop shaping. In such case, as suggested by [11], an LQG controller using simple weights can be designed and the resulting loop shape is used to aim for an H_∞ loop shaping. An alternative to H_∞ loop shaping is a standard H_∞ design with cost function such as S/KS sensitivity optimization.

The Syncrude utilities simulation model SYNSIM is used to model the utility boiler. The utility boiler model is obtained using N4SID identification method and RBS signal is used as perturbation on input side. The resulting model is used in the design of H-infinity controller for the proposed observer. The states estimated by the observer are then compared with the actual values given by SYNSIM. It should be noted that the SYNSIM is a first principle model, which provides some of those parameters that are not available for measurement in real plant. This is one of the many reasons why we use SYNSIM to model the boiler and also use it for comparison purposes.

Like most real plants, utility boiler is a non-linear process, which can be represented by linear model with in specified operating range. Because our design method is applicable only to linear plants, it seems difficult to extend our design method to non-linear processes. Here we take a simple approach of linearization to non-linear plant with in prescribed operating boundaries. We call this approach Observer Scheduling. The whole operating range is divided into three operating segments. It is assumed that the plant is linear with in the upper and lower limits of each operating segment. Boiler model is obtained for each operating segment and the resulting models are used to design observers for the respective operating segments. It can be seen that the observer designed for a particular operating segment works well if plant conditions are within the same operating segment while its performance is poor if the plant operates outside that segment. It is straightforward to monitor the error between the estimated output vector and the actual output vector for all observers and select the output of the observer that gives minimum error.

1.4 Literature Survey

Looking backward to the contribution of researchers to observer design and its application, a name D. Luenberger comes instantly in mind. In 1966 he presented the theory of observers for multivariable systems [12]. Most of the books on modern control theory refer this paper while discussing observer structures. The Observer structure proposed in this paper is widely known as Luenberger Observer. Luenberger Structure takes into consideration the deterministic properties of the system. This theory is true only if the plant-model mismatch is negligible.

State estimator known as Kalman filter, was proposed by R. E. Kalman [13] in 1960. One year later R.E. Kalman in collaboration with R.S. Bucy published another paper [14] regarding new results in state estimation. The usefulness of this theory can be evaluated by observing that control literature is full of research work related to Kalman Filtering. The Kalman filter is sensitive to parametric variations and requires a priori knowledge of noise statistics.

L. Xie and Y. C. Soh [15] extended Kalman filter theory to uncertain systems while Bernstein and W. Haddad [16] applied H_∞ theory to steady state Kalman filtering. I. R. Peterson and D. C. McFarlane [17] showed the change from conventional Kalman filter to a robust filter. It requires a minor modification to the filter structure to incorporate the uncertainty effect. The assumption of quadratic stability of uncertain system is a weak one, as it is rare that an estimator be applied ‘open loop’ to an unstable system [16].

R. Nikoukhah *et al.* [18] recently published a paper on the design of observer for general linear time-invariant systems. Jong-Koo Park [10] introduced a different approach of dynamic observer solution to state estimation.

The increasing use of fault detectors in different applications has directed an extensive study in the field of fault detection and isolation. Some of the first fault detection methods have been describe in the survey paper by A. S. Willsky [19]. A recent paper by Patton and Chen [20] gives a good overview of more modern model based fault detection. Such a study has been enhanced by the developments in modern control theory that has brought powerful techniques of mathematical modeling, H_2 and H_∞ optimal control and state estimation etc.

1.5 Contribution

In this thesis the concept of dynamic state estimator (input-output observer), for systems with plant-model mismatch and unknown disturbances and noise, is investigated. The analysis and design of input-output observer were carried out. The proposed estimator can be viewed as an extension of usual static estimator but the benefits of this extension are promising. One of the benefits is to transform the estimator design problem into H_∞ feedback controller design problem. This enables the designer to fully utilize the vast literature related to this theory. Using this method the designer can construct an effective estimator that will show desirable asymptotic properties and robustness. The performance limitations due to complexity such as right half plane zeros can be seen during the design process. In other observer designs it can only be noticed at later stages. The concept of observer scheduling is

introduced to tackle non-linearity. This approach suggests several observers for the whole operating range and switching to the suitable observer is done through some logic to get minimum error between estimated and actual state. Observer scheduling is easy to implement and due to the repetition of the design process, it is less time consuming.

1.6 Introduction to Syncrude Power Plant

Syncrude Canada Ltd. has a bitumen extraction and processing plant at Mildred Lake, Alberta. The 280 MW power plant, which supplies electrical energy as well as steam to the processing plant consists of five re-circulating gas fired boilers and two once through steam generators (OTSG's). These boilers supply up to 500 Kg/sec. of high-pressure steam to the main header, which is used for extraction, upgrading and generation of electrical and mechanical power. Three of the five re-circulating boilers are refinery gas fired boilers called Utility Boilers (UB's) while the remaining two are carbon mono-oxide gas fired boilers called CO Boilers (COB's). OTSG is like a conventional heat exchanger, which has two-phase flow in the inlet portion, saturated steam in the middle portion and superheated steam in the outlet portion. The Utility boilers are used to regulate pressure, CO boilers to regulate flow and OTSGs to regulate temperature. Four steam turbo-generators and two gas turbine generators are capable of generating up to 280 MW of electrical energy. Due to the limitation of steam supply, the additional load demand is met with the import of electrical energy via a tie line from Alberta Grid [1].

There are six turbine-generator sets. Out of which two are gas turbines and one is the condensing steam turbine while the remaining three are backpressure steam turbines. All the three, backpressure steam turbines take steam at 915psi from 900# header and discharge it into 50# header at approximately 50psi pressure.

The steam supply network consists of four headers. The 900psi high-pressure header, 600psi and 150psi medium-pressure headers and 50psi low-pressure header. The 600#, 150# and 50# headers supply steam to steam-distribution network. There are four steam letdown stations, 900-600# letdown, 600-150# letdown, 150-50# letdown and 600-50# letdown station. These letdown stations reduce the steam pressure and act as an interface between the headers of different pressures.

1.6.1 Utility Boiler

A steam boiler is one of the most important components in industrial plants such as power plants and chemical plants. Its operation has great impact on other parts of the plant. Failure of boiler may lead to a complete shutdown of the plant. Due to undesired dynamics such as time delays, non-linearity and inverse response characteristics of the boiler, it is considered one of the good examples in terms of industrial applications of theoretical concepts.

Each Utility boiler at Syncrude facility produces a nominal 94.5kg/sec. of steam at a pressure of 6.6 MPa (absolute) to a steam ring header. Feed water at a pressure of 6.6 MPa and flow rate of 94.5 Kg/sec is fed to the boiler. It is preheated in the economizer section from 141 °C to approximately 184 °C before it enters the steam drum. Water from the economizer outlet enters into the steam drum and then flows through the downcomers into the mud drum. The water from mud drum enters the

riser tubes, the slag screen and waterwalls. The waterwalls, slag screen and riser tubes collectively are called riser section. Water changes its state from liquid to saturated vapors in the riser section. The circulation of fluid in the boiler is due to the difference in density of the subcooled water in the downcomer and the saturated steam in the riser section respectively. The mixture of saturated steam with some portion of liquid enters the steam drum, where liquid is separated from saturated steam, and fed to the primary superheater and then to a secondary superheater. Steam is superheated at 510 °C in the two superheaters and is fed to the 900# common steam header. An attemperator is provided in between the two superheaters to control secondary superheater outlet steam temperature with the help of subcooled water spray. The spray flow is controlled through a cascade of temperature and spray flow controller [2].

Looking into the boiler from flue gas perspective, refinery gas is burnt in the combustion chamber called furnace and flue gases at a temperature of 1000 °C approximately are produced.

A significant amount of heat is absorbed through waterwalls and superheaters by radiation. The remaining energy is transferred to the other parts of the boiler due to convection. Hot flue gases from furnace enter secondary superheater and then primary superheater. The outlet of flue gas circuit of primary superheater is connected to the riser tubes and down comers. While transferring most of heat energy in the riser tube, flue gases enter economizer via downcomer, where the remaining heat energy is utilized to preheat the feed water. Finally relatively cool gas from the economizer enters exhaust section of the plant [2].

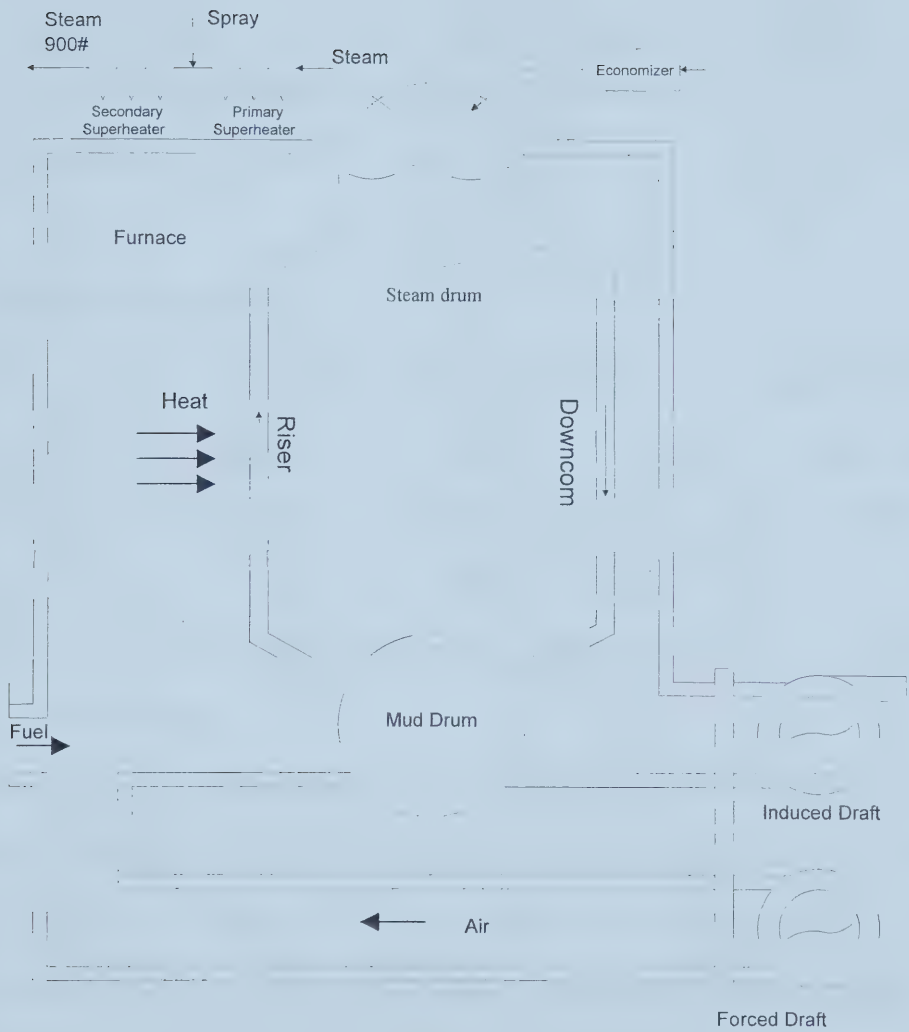


Figure 1.3: Natural Re-circulation Water Tube Boiler

The fuel used by utility boilers is the refinery gas that contains mainly methane, ethane and hydrogen. Fuel at 101.3 KPa and 25 °C is fed at the rate of approximately 5.5Kg/sec to the furnace section of the boiler where it is combusted with air. Air to fuel ratio is controlled such that the excess oxygen level in the flue gas leaving stack is 1.5mole% [2].

1.7 Thesis Organization

The rest of the thesis is organized as follows: In chapter 2, the proposed observer scheme called “Input-Output Observer” is discussed. The concept of input to state uncertainty is introduced. The mathematical expression in terms of “Observer Sensitivity Function” for input-output observer is derived. The stability of the observer structure under certain conditions is proved and properties of the proposed observer are discussed.

In chapter 3, by conducting a series of experiments on SYNSIM, linear models for Syncrude utility boiler under three different operating conditions are obtained. This is done to deal a non-linear process as linear, under specific operating conditions.

In chapter 4, observers are designed for utility boiler models obtained in chapter 3. The design is based on H_∞ loop shaping technique. Simulation results for comparison are given. The trade off between different specifications has been discussed and the strengths and weakness are identified.

Finally, in chapter 5, the problem encountered due to non-linearity of the process is discussed and the solution is provided through the introduction of observer bank. The performance of the observer bank through the entire operating range of the boiler is shown in the form of simulation results.

In chapter 6, a conclusion is drawn based on the results from previous chapters.

Chapter 2

Proposed Observer Scheme

In this chapter, a new observer scheme referred to as “Input-Output Observer” is introduced. The *input to state* approach to uncertainty as compared to *input to output* is introduced. The mathematical expression in terms of “Observer Sensitivity Function” is derived and important properties of the proposed observer structure are discussed.

The Robust Observer based on H-infinity control problem is proposed for state estimation to incorporate noise, disturbance and plant-model mismatch. The scheme proposed in [5] is followed and the structure of the observer and its mathematical analysis has been discussed. This observer structure is applied on real systems and its strength and weakness are discussed.

The classical approach to state estimation consists of an unforced system with nonzero initial conditions. The error dynamics are stabilized to achieve asymptotic convergence by designing the observer gain. In this type of approach it is difficult to incorporate modeling errors.

Robust estimation problem can be posed as robust control problem and so the design method is similar. Robust controller design results in a controller, which maintains its performance in the presence of model uncertainties. The relationship between state- space and input-output realization of dynamic system has played a great role in the success of robust controller design. Although the computations are performed in

state-space, modeling errors can be described in a better way using input-output structure. Most of the time, the amplitude of perturbation term is subject to frequency dependent bounds, which gives better insight into the dynamics of the system.

2.1 Input to State Uncertainty Approach

Here we emphasize the input-state approach to uncertainty problem. Systems are considered as mappings from input to state and the objective is a small estimation error in the presence of plant-model mismatch. A very general class of perturbation is imposed on the nominal plant to represent uncertainties. The observer can also be posed as a filter, such that the error dynamics ' \mathbf{e} ' is shaped according to desired frequency domain characteristics.

This observer under consideration is fundamentally different from the classical approach and as mentioned in [5] it has the following advantages:

1. It can easily handle unstructured uncertainties in the plant
2. Solution can be made optimal under worst-case exogenous perturbations.
3. It poses the robust observer problem as robust control problem thus taking advantage of the vast literature and software tools for the design.

We assume that $\mathbf{R}^{n \times n}$, $\mathbf{R}^{n \times p}$ and $\mathbf{R}^{q \times n}$ are a set of real matrices of the order $n \times n$, $n \times p$ and $q \times n$ respectively. Similarly $\mathbf{R}(s)$ is the set of proper rational functions of the form $\mathbf{f}(s)=\mathbf{n}(s)/\mathbf{d}(s)$, where $\mathbf{p}(s)$ and $\mathbf{d}(s)$ are polynomials in variable ' s ' with the degree of \mathbf{n} being at most equal to the degree of \mathbf{d} . $\mathbf{R}(s)^{p \times q}$ represents the set of matrices with elements in $\mathbf{R}(s)$. We will say that $\mathbf{F}(s) \in \mathbf{R}(s)^{p \times q}$ is a stability

matrix if and only if all the entries of **F** have poles in the left half of the complex plane [5].

Consider a system **P**, defined via minimal state space realization of the form **R**

$$\dot{\mathbf{x}} = \mathbf{Ax} + \mathbf{Bu} \dots \dots \dots (2.1)$$

$$\mathbf{y} = \mathbf{Cx} \dots \dots \dots (2.2)$$

Where $\mathbf{A} \in \mathbf{R}^{n \times n}$, $\mathbf{B} \in \mathbf{R}^{n \times p}$, and $\mathbf{C} \in \mathbf{R}^{q \times n}$

Here for simplicity we have assumed that **D = 0** in equation (2.2).

In the transfer function form **F** will be seen as input to state mapping and can be represented as:

$$\mathbf{F(s)} = (\mathbf{sI - A})^{-1} \mathbf{B} \dots \dots \dots (2.3)$$

$$\mathbf{P(s)} = \mathbf{CF(s)} = \mathbf{C(sI - A)^{-1}B} \dots \dots \dots (2.4)$$

The relationship between the two mappings is shown in figure 2.1.

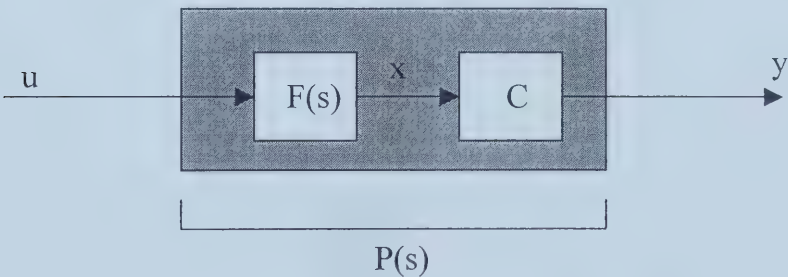


Figure 2.1: Relationship of system P with F and C

The above representation gives an excellent idea of how to deal states in an input-output domain. The system **F(s)** is defined as a system having **x** as output and **u** as input.

In robust control there are variety of ways to represent uncertainty. One of the popular approaches is to multiply the unstructured perturbation term with the input vector and add the resultant with the output vector. In our case we will multiply unstructured perturbation with the input vector but add the resultant with the state vector instead of the output vector. Our main objective is to estimate the state vector and it would be more logical to take into consideration the effect of uncertainty on states.

In Mathematical terms the plant $\mathbf{F}(s)$ including unstructured uncertainty can be represented as follows:

$$\mathbf{F}(s) = \mathbf{F}_o(s) + \Delta(s) \quad (2.5)$$

Where $\mathbf{F}_o(s) = (s\mathbf{I} - \mathbf{A})^{-1}\mathbf{B}$ and the perturbation term $\Delta(s)$ is an unknown but satisfies a frequency dependent bound

$$|\Delta(i\omega)| \leq \delta(i\omega) \quad \forall \omega \in \mathbf{R}$$

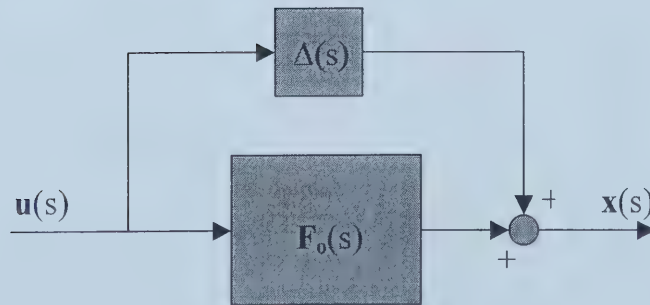


Figure 2.2: Uncertainty representation

2.2 An Input-Output Observer

Define the following structure, in the future referred to as an input-output observer

$$\hat{\mathbf{x}}(s) = \mathbf{F}_0(s) [\mathbf{u}(s) + \mathbf{G}(s)\mathbf{e}(s)] \quad (2.6)$$

$$\mathbf{e}(s) = \mathbf{y}(s) + \mathbf{n}(s) + \mathbf{d}(s) - \hat{\mathbf{y}}(s) \quad (2.7)$$

$$\hat{\mathbf{y}}(s) = \mathbf{C} \hat{\mathbf{x}}(s) \quad (2.8)$$

From figure 2.3 the following equations can be extracted

$$\mathbf{y}_m = \mathbf{y} + \mathbf{d} + \mathbf{n}$$

$$\Rightarrow \mathbf{y}_m = \{\mathbf{C} \mathbf{F}_0 \mathbf{u} + \mathbf{C} \Delta \mathbf{u}\} + \mathbf{d} + \mathbf{n}$$

$$\Rightarrow \mathbf{y}_m = \mathbf{C} \mathbf{F}_0 \mathbf{u} + \mathbf{C} \Delta \mathbf{u} + \mathbf{d} + \mathbf{n} \quad (2.9)$$

and

$$\mathbf{x}_r = \mathbf{F}_0 \mathbf{u} + \Delta \mathbf{u} \quad (2.10)$$

Also

$$\hat{\mathbf{x}} = \mathbf{F}_0 \mathbf{z}$$

$$\Rightarrow \hat{\mathbf{x}} = \mathbf{F}_0 (\mathbf{u} + \mathbf{G} \mathbf{e})$$

$$\Rightarrow \hat{\mathbf{x}} = \mathbf{F}_0 \mathbf{u} + \mathbf{F}_0 \mathbf{G} \mathbf{e} \quad (2.11)$$

Therefore

$$\hat{\mathbf{y}} = [\mathbf{I} + \mathbf{C} \mathbf{F}_0 \mathbf{G}]^{-1} (\mathbf{C} \mathbf{F}_0 \mathbf{u} + \mathbf{C} \mathbf{F}_0 \mathbf{G} \mathbf{y}_m)$$

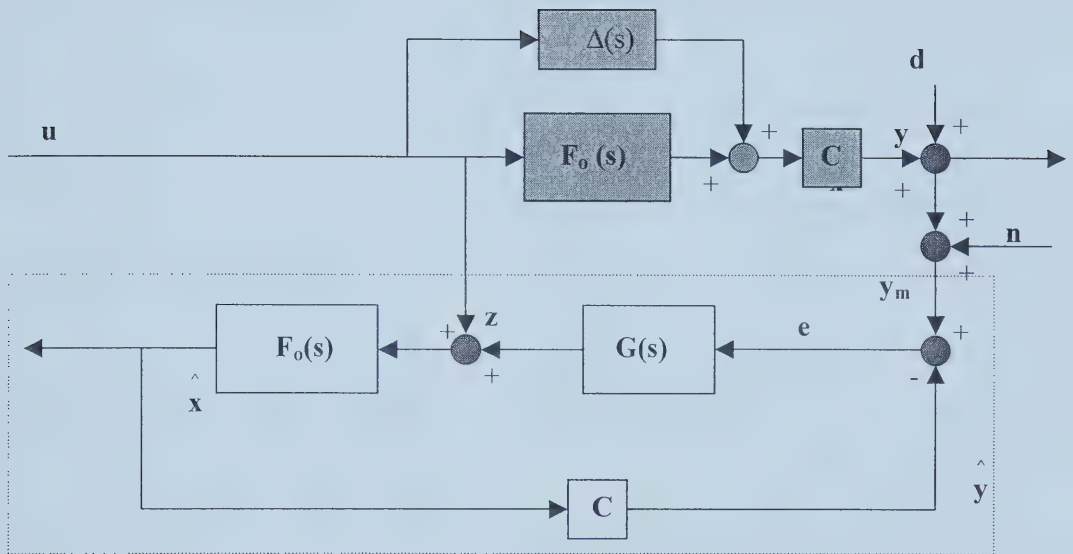


Figure 2.3: Input-Output Observer

If the error between the measured output and the estimated output is represented by \mathbf{e} then:

$$\begin{aligned}
 \mathbf{e} &= \mathbf{y}_m - \hat{\mathbf{y}} \\
 \Rightarrow \mathbf{e} &= \mathbf{y}_m - \left[\mathbf{I} + \mathbf{C F}_0 \mathbf{G} \right]^{-1} (\mathbf{C F}_0 \mathbf{u} + \mathbf{C F}_0 \mathbf{G y}_m) \\
 \Rightarrow \mathbf{e} &= \mathbf{y}_m - \left[\mathbf{I} + \mathbf{C F}_0 \mathbf{G} \right]^{-1} \mathbf{C F}_0 \mathbf{G y}_m - \left[\mathbf{I} + \mathbf{C F}_0 \mathbf{G} \right]^{-1} \mathbf{C F}_0 \mathbf{u} \\
 \Rightarrow \mathbf{e} &= \left[\mathbf{I} - \left\{ \mathbf{I} + \mathbf{C F}_0 \mathbf{G} \right\}^{-1} \mathbf{C F}_0 \mathbf{G} \right] \mathbf{y}_m - \left[\mathbf{I} + \mathbf{C F}_0 \mathbf{G} \right]^{-1} \mathbf{C F}_0 \mathbf{u} \quad (2.12)
 \end{aligned}$$

If \mathbf{A} is a square matrix of order $\mathbf{n} \times \mathbf{n}$ and \mathbf{I} is the identity matrix of the same order then it can be proved that :

$$\mathbf{I} - (\mathbf{I} + \mathbf{A})^{-1} = (\mathbf{I} + \mathbf{A})^{-1}$$

Using the above property, equation (2.12) can be written as:

$$\mathbf{e} = \left[\mathbf{I} + \mathbf{C F}_0 \mathbf{G} \right]^{-1} (\mathbf{y}_m - \mathbf{C F}_0 \mathbf{u}) \quad (2.13)$$

But from equation (2.9)

$$\mathbf{y}_m = \mathbf{C F}_0 \mathbf{u} + \mathbf{C} \Delta \mathbf{u} + \mathbf{d} + \mathbf{n}$$

Therefore equation (2.13) can be reduced to:

$$\mathbf{e} = \left[\mathbf{I} + \mathbf{C F}_0 \mathbf{G} \right]^{-1} (\mathbf{C} \Delta \mathbf{u} + \mathbf{d} + \mathbf{n}) \quad (2.14)$$

If $\tilde{\mathbf{x}}$ is defined as the error between actual and estimated state then we can write in mathematical terms as:

$$\tilde{\mathbf{x}} = \mathbf{x} - \hat{\mathbf{x}} \quad (2.15)$$

By substituting the value of \mathbf{x} and $\hat{\mathbf{x}}$ from eq.(2.10) and eq.(2.11) in eq.(2.15) we get:

$$\tilde{\mathbf{x}} = \Delta \mathbf{u} - \mathbf{F}_0 \mathbf{G} \mathbf{e} \quad (2.16)$$

Eq.(2.16) can be further elaborated by substituting the value of \mathbf{e} from eq.(2.14).

$$\tilde{\mathbf{x}} = \Delta \mathbf{u} - \mathbf{F}_0 \mathbf{G} \left[\mathbf{I} + \mathbf{C} \mathbf{F}_0 \mathbf{G} \right]^{-1} (\mathbf{C} \Delta \mathbf{u} + \mathbf{d} + \mathbf{n})$$

$$\Rightarrow \tilde{\mathbf{x}} = \Delta \mathbf{u} - \mathbf{F}_0 \mathbf{G} \left[\mathbf{I} + \mathbf{C} \mathbf{F}_0 \mathbf{G} \right]^{-1} \mathbf{C} \Delta \mathbf{u} - \mathbf{F}_0 \mathbf{G} \left[\mathbf{I} + \mathbf{C} \mathbf{F}_0 \mathbf{G} \right]^{-1} (\mathbf{d} + \mathbf{n})$$

Define

$$\tilde{\mathbf{x}}_1 = \Delta \mathbf{u} - \mathbf{F}_0 \mathbf{G} \left[\mathbf{I} + \mathbf{C} \mathbf{F}_0 \mathbf{G} \right]^{-1} \mathbf{C} \Delta \mathbf{u} \quad (2.17)$$

$$\tilde{\mathbf{x}}_2 = -\mathbf{F}_0 \mathbf{G} \left[\mathbf{I} + \mathbf{C} \mathbf{F}_0 \mathbf{G} \right]^{-1} (\mathbf{d} + \mathbf{n}) \quad (2.18)$$

Therefore

$$\tilde{\mathbf{x}} = \tilde{\mathbf{x}}_1 + \tilde{\mathbf{x}}_2 \quad (2.19)$$

To simplify eq.(2.17) consider a system having transfer function blocks \mathbf{G}_1 , \mathbf{G}_2 , \mathbf{H}_1 and \mathbf{H}_2 , interconnected as shown in figure 2.4. The output \mathbf{Y} can be represented as :

$$\mathbf{Y} = \left[\left\{ \mathbf{I} + \mathbf{G}_2 \mathbf{G}_1 \mathbf{H}_2 \mathbf{H}_1 \right\}^{-1} \mathbf{G}_2 \mathbf{G}_1 \right] \mathbf{R} \quad (2.20)$$

$$\text{But } \mathbf{Y} = \left[\mathbf{G}_2 \mathbf{G}_1 - \mathbf{G}_2 \mathbf{G}_1 \mathbf{H}_2 \left\{ \mathbf{I} + \mathbf{H}_1 \mathbf{G}_2 \mathbf{G}_1 \mathbf{H}_2 \right\}^{-1} \mathbf{G}_2 \mathbf{G}_1 \right] \mathbf{R} \quad (2.21)$$

Therefore from eq.(2.20) and eq.(2.21) we get:

$$\left\{ \mathbf{I} + \mathbf{G}_2 \mathbf{G}_1 \mathbf{H}_2 \mathbf{H}_1 \right\}^{-1} \mathbf{G}_2 \mathbf{G}_1 = \mathbf{G}_2 \mathbf{G}_1 - \mathbf{G}_2 \mathbf{G}_1 \mathbf{H}_2 \left\{ \mathbf{I} + \mathbf{H}_1 \mathbf{G}_2 \mathbf{G}_1 \mathbf{H}_2 \right\}^{-1} \mathbf{G}_2 \mathbf{G}_1$$

(See problem 4.3 in [6], page 141)

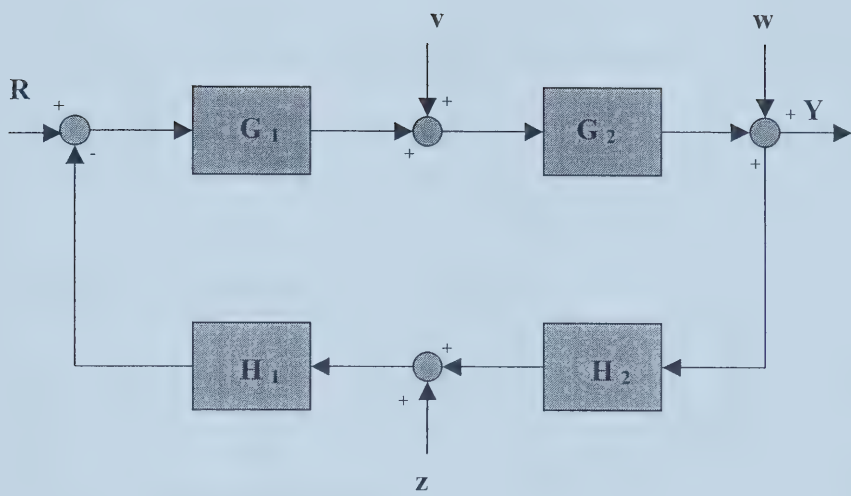


Figure 2.4: Interconnected System

By using the above result eq.(2.17) becomes:

$$\tilde{\mathbf{x}}_1 = \left[\mathbf{I} + \mathbf{F}_0 \mathbf{G} \mathbf{C} \right]^{-1} \Delta \mathbf{u} \quad (2.22)$$

Now consider two matrices A and B such that inverse of (I+AB) exists then according matrix properties

$$\mathbf{B} (\mathbf{I} + \mathbf{AB})^{-1} = (\mathbf{I} + \mathbf{BA})^{-1} \mathbf{B}$$

Using the result mentioned above, eq.(2.18) can be re-written as:

$$\tilde{\mathbf{x}}_2 = - \left[\mathbf{I} + \mathbf{F}_0 \mathbf{G} \mathbf{C} \right]^{-1} \mathbf{F}_0 \mathbf{G} (\mathbf{d} + \mathbf{n}) \quad (2.23)$$

By the combination of eq.(2.22) and eq.(2.23) we get:

$$\tilde{\mathbf{x}} = \left[\mathbf{I} + \mathbf{F}_0 \mathbf{G} \mathbf{C} \right]^{-1} \left\{ \Delta \mathbf{u} - \mathbf{F}_0 \mathbf{G} (\mathbf{d} + \mathbf{n}) \right\} \quad (2.24)$$

$$\Rightarrow \tilde{\mathbf{x}} = \mathbf{H} \left\{ \Delta \mathbf{u} - \mathbf{F}_0 \mathbf{G} (\mathbf{d} + \mathbf{n}) \right\} \quad (2.25)$$

Where:

$$\mathbf{H} = \left[\mathbf{I} + \mathbf{F}_0 \mathbf{G} \mathbf{C} \right]^{-1}$$

and is called the “*observer sensitivity*”. The problem now is to minimize the state error $\tilde{\mathbf{x}}$ by minimizing the sensitivity function \mathbf{H} for uncertainty and $\mathbf{H}\mathbf{F}_0\mathbf{G}$ for disturbance and noise. This can be achieved by finding an optimal compensator $\mathbf{G}(s)$ to satisfy a set of frequency dependent specifications on the observer sensitivity $\mathbf{H}(s)$.

2.3 Observer Stability

One of the basic requirements is to ensure the stability of the observer. Define the feedback system \mathbf{S}_1 as shown in figure 2.5.

For the system \mathbf{S}_1 define the mapping $\mathbf{M}_1(s)$ as follows:

$$\begin{pmatrix} \mathbf{e}_1 \\ \mathbf{e}_2 \end{pmatrix} = \mathbf{M}_1(s) \begin{pmatrix} \mathbf{u}_1 \\ \mathbf{u}_2 \end{pmatrix}$$

$$\begin{pmatrix} \mathbf{e}_1 \\ \mathbf{e}_2 \end{pmatrix} = \begin{bmatrix} (\mathbf{I} + \mathbf{C}\mathbf{F}_0\mathbf{G})^{-1} & (\mathbf{I} + \mathbf{C}\mathbf{F}_0\mathbf{G})^{-1}\mathbf{C}\mathbf{F}_0 \\ (\mathbf{I} + \mathbf{G}\mathbf{C}\mathbf{F}_0)^{-1}\mathbf{G} & (\mathbf{I} + \mathbf{G}\mathbf{C}\mathbf{F}_0)^{-1} \end{bmatrix} \begin{pmatrix} \mathbf{u}_1 \\ \mathbf{u}_2 \end{pmatrix}$$

The system \mathbf{S}_1 shown in figure 2.5 corresponds to the feedback loop of the observer structure defined in eq.(2.6) to eq.(2.8).

Assume that the observer blocks \mathbf{F}_0 and \mathbf{G} are defined via state space realization $\boldsymbol{\phi}_1$ and $\boldsymbol{\phi}_2$, respectively where:

$$\begin{aligned} \boldsymbol{\phi}_1: \quad \dot{\hat{\mathbf{x}}} &= \mathbf{A} \hat{\mathbf{x}} + \mathbf{B}\mathbf{e}_2 \\ \Rightarrow \dot{\hat{\mathbf{x}}} &= \mathbf{A} \hat{\mathbf{x}} + \mathbf{B}(\mathbf{u}_2 + \mathbf{y}_1) \end{aligned} \tag{2.26}$$

$$\hat{\mathbf{y}} = \mathbf{C} \hat{\mathbf{x}} \tag{2.27}$$

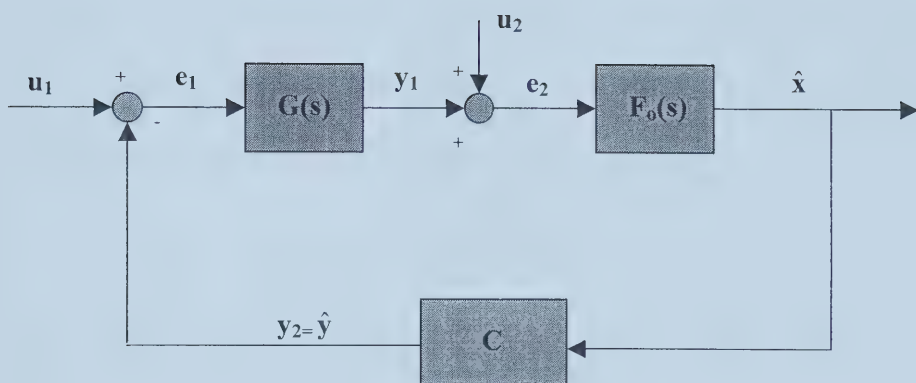


Figure 2.5: The System S1

$$\Phi_2: \quad \dot{\mathbf{x}}_1 = \mathbf{A}_1 \mathbf{x}_1 + \mathbf{B}_1 \mathbf{e}_1$$

$$\Rightarrow \dot{\mathbf{x}}_1 = \mathbf{A}_1 \mathbf{x}_1 + \mathbf{B}_1 (\mathbf{u}_1 - \hat{\mathbf{y}}) \quad (2.28)$$

$$\mathbf{y}_1 = \mathbf{C}_1 \mathbf{x}_1 \quad (2.29)$$

Theorem 1:

(Taken from [5])

Assuming that F_0 and G are defined via controllable and observable state space realization Φ_1 and Φ_2 of the form eq.(2.26) to eq.(2.29), then the input-output observer is internally stable if and only if the matrix

$$\overline{\mathbf{A}} = \begin{bmatrix} \mathbf{A} & \mathbf{B}\mathbf{C}_1 \\ -\mathbf{B}_1\mathbf{C} & \mathbf{A}_1 \end{bmatrix}$$

has all of its eigenvalues in the open right half plane.

Proof:

Define $\overline{\mathbf{x}} = (\hat{\mathbf{x}}, \mathbf{x}_1)^T$

$$\dot{\overline{\mathbf{x}}} = \begin{pmatrix} \dot{\hat{\mathbf{x}}} \\ \dot{\mathbf{x}}_1 \end{pmatrix} = \begin{pmatrix} \mathbf{A} & \mathbf{B}\mathbf{C}_1 \\ -\mathbf{B}_1\mathbf{C} & \mathbf{A}_1 \end{pmatrix} \begin{pmatrix} \hat{\mathbf{x}} \\ \mathbf{x}_1 \end{pmatrix} + \begin{pmatrix} \mathbf{0} & \mathbf{B} \\ \mathbf{B}_1 & \mathbf{0} \end{pmatrix} \begin{pmatrix} \mathbf{u}_1 \\ \mathbf{u}_2 \end{pmatrix}$$

$$\begin{pmatrix} \mathbf{y}_1 \\ \mathbf{y}_2 \end{pmatrix} = \begin{pmatrix} \mathbf{0} & \mathbf{C}_1 \\ \mathbf{C} & \mathbf{0} \end{pmatrix} \begin{pmatrix} \hat{\mathbf{x}} \\ \mathbf{x}_1 \end{pmatrix}$$

Or

$$\dot{\overline{\mathbf{x}}} = \overline{\mathbf{A}}\overline{\mathbf{x}} + \overline{\mathbf{B}}\mathbf{u} \quad (2.30)$$

$$\overline{\mathbf{y}} = \overline{\mathbf{C}}\overline{\mathbf{x}} \quad (2.31)$$

It is clear that if $\overline{\mathbf{A}}$ has no eigenvalues in the closed RHP, then \mathbf{M}_1 is a stability matrix. For the converse, notice that with $\boldsymbol{\phi}_1$ and $\boldsymbol{\phi}_2$ controllable and observable, the state space realization eq.(2.30) and eq.(2.31) of the feedback system \mathbf{S}_1 is also controllable and observable(see for example [7], page 446).

To analyze the error dynamics it is convenient to introduce an additional input to the feedback system of figure 2.5, as shown in the figure 2.6. Let this system be denoted by \mathbf{S}_2 .

As with the system \mathbf{S}_1 , we define $\mathbf{M}_2(s)$ as follows:

$$\begin{pmatrix} \mathbf{e}_1 \\ \mathbf{e}_2 \\ \mathbf{e}_3 \end{pmatrix} = \mathbf{M}_2(s) \begin{pmatrix} \mathbf{u}_1 \\ \mathbf{u}_2 \\ \mathbf{u}_3 \end{pmatrix} \quad (2.32)$$

$$\begin{pmatrix} \mathbf{e}_1 \\ \mathbf{e}_2 \\ \mathbf{e}_3 \end{pmatrix} = \begin{pmatrix} (\mathbf{I} + \mathbf{C}\mathbf{F}_0\mathbf{G})^{-1} & (\mathbf{I} + \mathbf{C}\mathbf{F}_0\mathbf{G})^{-1}\mathbf{C}\mathbf{F}_0 & (\mathbf{I} + \mathbf{C}\mathbf{F}_0\mathbf{G})^{-1}\mathbf{C} \\ (\mathbf{I} + \mathbf{G}\mathbf{C}\mathbf{F}_0)^{-1}\mathbf{G} & (\mathbf{I} + \mathbf{G}\mathbf{C}\mathbf{F}_0)^{-1} & (\mathbf{I} + \mathbf{G}\mathbf{C}\mathbf{F}_0)^{-1}\mathbf{G}\mathbf{C} \\ (\mathbf{I} + \mathbf{F}_0\mathbf{G}\mathbf{C})^{-1}\mathbf{F}_0\mathbf{G} & (\mathbf{I} + \mathbf{F}_0\mathbf{G}\mathbf{C})^{-1}\mathbf{F}_0 & (\mathbf{I} + \mathbf{F}_0\mathbf{G}\mathbf{C})^{-1} \end{pmatrix} \begin{pmatrix} \mathbf{u}_1 \\ \mathbf{u}_2 \\ \mathbf{u}_3 \end{pmatrix}$$

We will denote the entries of this matrix by \mathbf{M}_2^{ij} . The following lemma (Lemma 4.1 from [5]) says that the addition of the input \mathbf{u}_3 does not affect the internal stability of \mathbf{S}_1 .

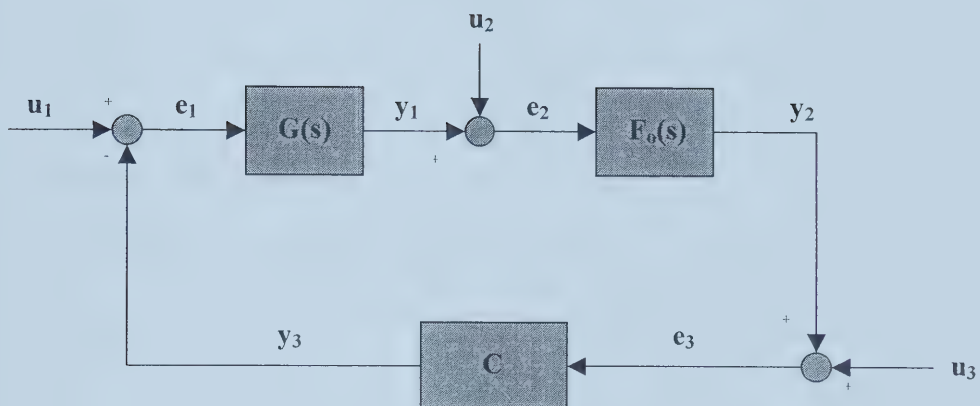


Figure 2.6: The System S2

Lemma:

The feedback system **S1** is internally stable if and only if the system **S2** is internally stable.

Which means that the matrices

$$\mathbf{M}_2^{33} = (\mathbf{I} + \mathbf{F}_0 \mathbf{G} \mathbf{C})^{-1}$$

and

$$\mathbf{M}_2^{31} = (\mathbf{I} + \mathbf{F}_0 \mathbf{G} \mathbf{C})^{-1} \mathbf{F}_0 \mathbf{G}$$

are stable matrices.

2.4 Observer Properties:

1. Since $(\mathbf{I} + \mathbf{F}_0 \mathbf{G} \mathbf{C})^{-1}$ and $(\mathbf{I} + \mathbf{F}_0 \mathbf{G} \mathbf{C})^{-1} \mathbf{F}_0 \mathbf{G}$ are stable matrices by assumption therefore bounded inputs (u , n , & d) will lead to a bounded estimation error.
2. From eq. (2.25) it can easily be concluded that in the absence of noise and disturbances ($n + d = 0$) and without modeling error ($\Delta = \mathbf{0}$), $\tilde{\mathbf{x}}$ is identically zero, provided that the input-output observer is internally stable. This conclusion is consistent with our input-output analysis, which ignores the effect of possible non-zero initial conditions.
3. Small estimation errors can be achieved by finding a compensator $G(s)$ which:
 - a) stabilizes the observer
 - b) minimize the error equation with the respect to uncertainties, noise and disturbances of known frequency content.

This is a standard problem, which can be cast in the context of \mathbf{H}_∞ framework.

While the exact solution of minimization is still unknown, the problem can be solved indirectly by minimizing the following norm:

$$\|\Phi\|_\infty = \left\| \frac{\mathbf{W}_1(\mathbf{I} + \mathbf{F}_0\mathbf{G}\mathbf{C})^{-1}}{\mathbf{W}_2(\mathbf{I} + \mathbf{F}_0\mathbf{G}\mathbf{C})^{-1}\mathbf{F}_0\mathbf{G}} \right\|_\infty \quad (2.33)$$

Where \mathbf{W}_1 and \mathbf{W}_2 are weighting functions. This approach is taken from [5] and [8].

4. Initial conditions can be included as follows:

Assume that n , d and Δ are identically zero in figure 2.3 and consider minimal state space realization of \mathbf{F}_0 and \mathbf{G} . With the notation of figure 2.3, we have:

The Plant: $\dot{\mathbf{x}} = \mathbf{A}\mathbf{x} + \mathbf{B}\mathbf{u}$

$$\mathbf{y} = \mathbf{C}\mathbf{x}$$

Observer Block \mathbf{F}_0 : $\dot{\hat{\mathbf{x}}} = \mathbf{A}\hat{\mathbf{x}} + \mathbf{B}(\mathbf{z} + \mathbf{u})$

$$\hat{\mathbf{y}} = \mathbf{C}\hat{\mathbf{x}}$$

Observer Block \mathbf{G} : $\dot{\mathbf{x}}_1 = \mathbf{A}_1\mathbf{x}_1 + \mathbf{B}_1(\mathbf{y} - \hat{\mathbf{y}})$

$$\mathbf{y}_1 = \mathbf{C}_1\mathbf{x}_1$$

It follows that

$$\tilde{\dot{\mathbf{x}}} = \dot{\hat{\mathbf{x}}} - \dot{\mathbf{x}}$$

$$\Rightarrow \tilde{\dot{\mathbf{x}}} = (\mathbf{A}\hat{\mathbf{x}} + \mathbf{B}\mathbf{u} + \mathbf{B}\mathbf{C}_1\mathbf{x}_1) - (\mathbf{A}\mathbf{x} + \mathbf{B}\mathbf{u})$$

$$\Rightarrow \tilde{\dot{\mathbf{x}}} = \mathbf{A}(\hat{\mathbf{x}} - \mathbf{x}) + \mathbf{B}\mathbf{C}_1\mathbf{x}_1$$

$$\Rightarrow \tilde{\dot{\mathbf{x}}} = \mathbf{A}\tilde{\mathbf{x}} + \mathbf{B}\mathbf{C}_1\mathbf{x}_1 \quad (2.34)$$

Also

$$\begin{aligned}
\dot{\mathbf{x}}_1 &= \mathbf{A}_1 \mathbf{x}_1 + \mathbf{B}_1 \mathbf{C} \mathbf{x} - \mathbf{B}_1 \mathbf{C} \hat{\mathbf{x}} \\
\Rightarrow \dot{\mathbf{x}}_1 &= \mathbf{A}_1 \mathbf{x}_1 - \mathbf{B}_1 \mathbf{C} (\hat{\mathbf{x}} - \mathbf{x}) \\
\Rightarrow \dot{\mathbf{x}}_1 &= \mathbf{A}_1 \mathbf{x}_1 - \mathbf{B}_1 \mathbf{C} \tilde{\mathbf{x}}
\end{aligned} \tag{2.35}$$

Defining

$$\mathcal{X}^* = \begin{pmatrix} \tilde{\mathbf{x}} \\ \mathbf{x}_1 \end{pmatrix}$$

We have that

$$\dot{\mathcal{X}}^* = \begin{pmatrix} \dot{\tilde{\mathbf{x}}} \\ \dot{\mathbf{x}}_1 \end{pmatrix} = \begin{pmatrix} \mathbf{A} & \mathbf{B} \mathbf{C}_1 \\ -\mathbf{B}_1 \mathbf{C} & \mathbf{A}_1 \end{pmatrix} \begin{pmatrix} \tilde{\mathbf{x}} \\ \mathbf{x}_1 \end{pmatrix} \tag{2.36}$$

$$\dot{\mathcal{X}}^* = \overline{\mathbf{A}} \mathcal{X}^* \tag{2.37}$$

and since the eigenvalues of $\overline{\mathbf{A}}$ are in the left half plane, it follows that $\hat{\mathbf{x}}$ will asymptotically converges to \mathbf{x} . Thus the input-output can be seen as asymptotic observer, the same property as that of Luenberger observer.

2.5 Comments:

As posed this problem can be solved if and only if $\mathbf{F}_0 \mathbf{G}$ is a square matrix. This means that the minimization problem described in eq.(2.33) is solvable if and only if the dimension of the output is equal to the number of states.

A physical interpretation of this result is the following:

It is well known in control systems that in order to minimize the sensitivity of parametric variation on certain variables, that variable must be measured and

feedback to the controller (see for example: Kwakernak-Sivan). This fact is supported by Vidyasagar [34] in the following words. “ *For flat plant case the sensitivity minimization problem for multivariable is much deeper than the corresponding problem for scalar systems. At present the clean solution to the problem is available only in the case where the plant has at least as many inputs as outputs*”. In our case it means that we need to measure as many outputs as the number of states.

In order to proceed and shape the observer, we will concentrate on the minimization of $[\mathbf{I} + \mathbf{C}\mathbf{F}_0\mathbf{G}]^{-1}$, which is square and is solvable.

Some of the negative points associated with this method are:

1. Weighting functions are tough to choose and are time consuming.
2. The filter or the controller part of the observer, obtained as a result of the design, is high order. The order would always be at least equal to or greater than the order of the plant.
3. Luenberger observer is good in the speed of a response, and can be a better choice if frequency response characteristic is not an issue.

Chapter 3

Model Identification

This chapter presents the development of a “Boiler System” model carried on the basis of N4SID (Numerical Sub Space State Space **I**dentification) method. Linear models under three different operating conditions are obtained by conducting several experiments on SYNSIM. Finally, the time domain responses of the resultant models are compared with the response given by SYNSIM .

The resulting models are linear and include inverse response (Shrink and Swell effects) and time delays. The behavior of these models in this chapter represents the significant dynamics of the boiler system at Syncrude power plant.

Modeling issues associated with multi-input, multi-output (MIMO) systems have long been a significant focus of attention by academics and control practitioners alike. Even if a MIMO identification is technically sound, ease of use and reduction of risk to plant operations due to its application always remain a pressing issue. Therefore the development of “simple and convenient” methods for identification is considered as important area in the control research community. In addition to ease of design considerations, “plant friendliness” during experimental testing for identification has always been a concern among the practicing control engineers. The term “plant friendliness” means getting a suitable model in a shortest possible time while keeping the variation in the input and output parameters within the acceptable limits. In practice it is the compromise between the demands of a theory and the restrictions

placed by plant engineers who always prefer minimum perturbation imposed on the process.

Historically the models of choice in early industrial applications were time domain, input/output, step, or impulse response models. It was probably due to the ease of understanding provided by this form. With the advent of multivariable approach in control theory, state-space became the focus of attention. State-space model has several advantages, including easy generalization to multivariable systems, ease of analysis of closed loop properties, and online computation. In addition, with this model form, the wealth of systems theory - the linear quadratic (LQ) regulator theory, Kalman filtering theory, and H-infinity theory, etc. - is immediately available for use.

3.1 Objective and methodology:

The objective and application of the required model is a key factor in selecting the type of model and the method of identification. In our case, the objective is to find a simple linear model in a mathematical form suitable to use for observer design.

SYNSIM - the non-linear matlab-simulink based model for Syncrude utilities plant - is available due to work done as part of previous phase of the same project. The utility boiler model and the associated control system models are available as a simulink blocks inside SYNSIM. Due to the mathematical complexity and high interaction between different blocks, it is difficult to represent it in a simple mathematical form. For that purpose some identification techniques need to be applied to get a simple linear model. First approach is to perform tests on actual system and collect input-output data. In performing experiments for the purpose of

identification. several parameters, such as sampling rate and type of input signal, are chosen after several and repetitive tests. The number and duration of these tests depend on the complexity of the system and/or the lack of prior knowledge about the process. In our case, due to the operational constraints such as high interconnectivity of utility boiler with the rest of the plant, some tests are either practically not possible or difficult to perform. Specially keeping the plant under perturbation for long time is a risky job and needs tremendous efforts to convince plant operators.

To avoid delay due to operational and administrative constraints, another approach is considered for the purpose of study only. Assuming that SYNSIM represents the actual plant with high degree of confidence and that the dynamics of utility boiler and associated control system with in SYNSIM exactly replicate the dynamics of the actual system. The data collection experiments are performed on SYNSIM and a model is obtained based on the above assumption. In simple terms we consider SYNSIM as a plant. From now onward, the term “plant” will be used for SYNSIM simulation model.

3.2 Numerical Sub-Space State Space Identification:

System identification is usually concerned with computing polynomial models which some times give rise to highly ill-conditioned mathematical problems, especially for multi-input, multi-output systems. Numerical algorithms for subspace state space identification (N4SID) are better alternative in this kind of situations. This is especially true for high order multivariable systems, for which it is not trivial to find useful parameterization among all possible parameterization. With N4SID algorithms, most of this a priori parameterization can be avoided. Only the order of the system is

needed and it can be determined through inspection of the dominant singular values of a matrix that is calculated during the identification.

Another major advantage is that N4SID algorithms are non-iterative, with no non-linear optimization part involved. That is why they do not suffer from typical disadvantages of iterative algorithms, e.g. no guaranteed conversion, local minima of the objective criterion and sensitivity to initial estimates.

For classical identification, an extra parameterization of the initial state is needed when estimating a state space system from data measured on a plant with a non-zero initial condition. The advantage of the N4SID algorithm is that there is no difference between zero and non-zero initial states. In short, N4SID algorithms are always convergent (non-iterative) and numerically stable since they only make use of QR and singular value decomposition [8].

In addition to the above advantages, the reason why this method is selected, is the state space nature of the resultant model, required for state estimation, and the commercial availability of N4SID algorithm as a part of Matlab Identification toolbox.

3.3 Selection of input-output parameters:

The outputs of the Boiler system (including the associated control) at Syncrude utility plant are:

- a) Drum pressure
- b) Drum level
- c) Steam Temperature

There are three parameters, which are available in SYNSIM, but could not be measured in practice. Those are the following:

- (a) Furnace gas temperature
- (b) Super Heater gas temperature
- (c) Economizer gas temperature

The requirement is to estimate these three unmeasured parameters by measuring the outputs. This might be possible if a model is identified with the number of states equal to or higher than three and the parameters of interest, namely, furnace gas temperature, super heater gas temperature and economizer gas temperature are part of the states. Any state estimation technique can then be applied to estimate the parameters in question.

The inputs to the boiler system are:

- a) Steam load
- b) Feed water temperature
- c) Feed water pressure

Output response to step changes in the input parameters revealed that two parameters, feed water temperature and feed water pressure, have almost no effect while steam load has significant effect on outputs. This reduces the number of inputs to one. Considering the fact that for state estimation only one output is sufficient provided the observability condition is satisfied. Therefore, out of three, we take one output that will serve our purpose. Drum pressure being the most important output and accurately measurable is chosen as output of the system. The multi-input multi-output problem is reduced to a single-input single-output system.

3.4 Physical Interpretation of States:

Model obtained by using identification technique is a black box model with states having no physical interpretation. The only method to get a state space model with states representing any physical parameter of the process is the first principle method. Due to complexity and non-linearity of the actual process and the limited time for this particular job in the project, a different approach is considered. By taking advantage of the SYNSIM, a black box model is identified with four outputs and one input. The original model is transformed into another model with one input, one output and three states.

The input is:

$$u = \text{steam load}$$

The four outputs are:

$$y_1 = \text{furnace gas temperature}$$

$$y_2 = \text{Super heater gas temperature}$$

$$y_3 = \text{economizer gas temperature}$$

$$y_4 = \text{drum pressure}$$

Now define the following vectors and matrices:

$$\mathbf{Y}_{14} = [y_1 \ y_2 \ y_3 \ y_4]^T, \mathbf{Y}_{13} = [y_1 \ y_2 \ y_3]^T, \mathbf{X}_{13} = [x_1 \ x_2 \ x_3]^T$$

$$\mathbf{D}_{14} = [d_1 \ d_2 \ d_3 \ d_4]^T, \mathbf{C}_4 = [c_{41} \ c_{42} \ c_{43}]^T, \mathbf{B}_{13} = [b_1 \ b_2 \ b_3]^T$$

$$\mathbf{D}_{13} = [d_1 \ d_2 \ d_3]^T, \mathbf{D}_4 = [d_4], \mathbf{y}_4 = [y_4]$$

$$\mathbf{A}_{13} = \begin{bmatrix} a_{11} & a_{12} & a_{13} \\ a_{21} & a_{22} & a_{23} \\ a_{31} & a_{32} & a_{33} \end{bmatrix}, \mathbf{C}_{14} = \begin{bmatrix} c_{11} & c_{12} & c_{13} \\ c_{21} & c_{22} & c_{23} \\ c_{31} & c_{32} & c_{33} \\ c_{41} & c_{42} & c_{43} \end{bmatrix}, \mathbf{C}_{13} = \begin{bmatrix} c_{11} & c_{12} & c_{13} \\ c_{21} & c_{22} & c_{23} \\ c_{31} & c_{32} & c_{33} \end{bmatrix}$$

The model identified is in the form:

$$\dot{\mathbf{X}}_{13} = \mathbf{A}_{13}\mathbf{X}_{13} + \mathbf{B}_{13}u \quad (3.1)$$

$$\mathbf{Y}_{14} = \mathbf{C}_{14}\mathbf{X}_{13} + \mathbf{D}_{14}u \quad (3.2)$$

The vector \mathbf{y}_{14} is split into two parts \mathbf{y}_{13} and \mathbf{y}_4

$$\mathbf{Y}_{13} = \mathbf{C}_{13}\mathbf{X}_{13} + \mathbf{D}_{13}u \quad (3.3)$$

$$\mathbf{Y}_4 = \mathbf{C}_4\mathbf{X}_{13} + \mathbf{D}_4u \quad (3.4)$$

If $(\mathbf{C}_{13})^{-1}$ exists then eq. (3.3) can be re-written as:

$$\mathbf{X}_{13} = (\mathbf{C}_{13})^{-1}[\mathbf{Y}_{13} - \mathbf{D}_{13}u] \quad (3.5)$$

Let $[\mathbf{Y}_{13} - \mathbf{D}_{13}u] = \mathbf{Z} = [z_1 \ z_2 \ z_3]^T$, then:

$$\mathbf{X}_{13} = (\mathbf{C}_{13})^{-1}\mathbf{Z} \quad (3.6)$$

By substituting the value of \mathbf{X}_{13} from eq. (3.6) in eq. (3.1) and eq. (3.4) we get:

$$\begin{aligned} (\mathbf{C}_{13})^{-1}\dot{\mathbf{Z}} &= \mathbf{A}_{13}(\mathbf{C}_{13})^{-1}\mathbf{Z} + \mathbf{B}_{13}u \\ \Rightarrow \dot{\mathbf{Z}} &= \mathbf{C}_{13}\mathbf{A}_{13}(\mathbf{C}_{13})^{-1}\mathbf{Z} + \mathbf{C}_{13}\mathbf{B}_{13}u \end{aligned} \quad (3.7)$$

And also

$$\mathbf{Y}_4 = \mathbf{C}_4(\mathbf{C}_{13})^{-1}\mathbf{Z} + \mathbf{D}_4u \quad (3.8)$$

Define $\mathbf{A} = \mathbf{C}_{13}\mathbf{A}_{13}(\mathbf{C}_{13})^{-1}$, $\mathbf{B} = \mathbf{C}_{13}\mathbf{B}_{13}$, $\mathbf{C} = \mathbf{C}_4(\mathbf{C}_{13})^{-1}$, $\mathbf{D} = \mathbf{D}_4$, and $\mathbf{Y} = \mathbf{Y}_4$.

Equation (3.7) and (3.8) can be written as:

$$\dot{\mathbf{Z}} = \mathbf{AZ} + \mathbf{Bu} \quad (3.9)$$

$$\mathbf{Y} = \mathbf{CZ} + \mathbf{Du} \quad (3.10)$$

$\mathbf{Z} = [z_1 \ z_2 \ z_3]^T$ does not have a physical meaning but $\mathbf{Y}_{13} = [y_1 \ y_2 \ y_3]^T$ is the linear combination of \mathbf{Z} and u and can be calculated after estimation of vector \mathbf{Z} .

$$\mathbf{Y}_{13} = \mathbf{Z} + \mathbf{D}_{13} u \quad (3.11)$$

$$\mathbf{Y}_{13} = \begin{bmatrix} y_1 \\ y_2 \\ y_3 \end{bmatrix} = \begin{bmatrix} \text{Furnace gas temperature} \\ \text{Superheater gas temperature} \\ \text{Economizer gas temperature} \end{bmatrix} \quad (3.12)$$

3.5 Input Signal Design:

The input signal used for excitation can have a significant influence on the resulting parameter estimates. The choice of input depends on the type of identification method. For example, the transient analysis requires a step or impulse as input, while correlation analysis generally uses a pseudo-random binary signal. In other cases, the input may be chosen in another way and the problem of choosing a suitable signal becomes an important aspect of system identification. From a control point of view, all plant modes need not to be excited in the experiment. It is important, however, to

include information to the cross over frequency of the loop transfer function, which usually corresponds to the closed loop bandwidth [9].

Experience has proved that Pseudo-random Binary Signal (PRBS) and Random Binary Signal (RBS) give good results in cases where plant is linear with in some bounds. PRBS or RBS is a signal that shifts between two levels in a certain fashion. The difference between PRBS and RBS is that PRBS is a periodic while RBS is non-periodic signal. PRBS need additional parameter to be specified, the repetition time, i.e. after how much time PRBS should repeat its sequence, which requires *a priori* knowledge of the process. As a matter of simplicity and without any compromise on the quality of the experiment, an RBS is chosen as input for our experiment. The only tricky part here is to specify the range of frequencies over which the dynamics of system need to be captured.

The matlab “System identification toolbox” command “*Idinput*” is used to generate the signal. Keeping in view the large settling time of the process, the frequency range between ‘0’ and 0.01 is selected. The magnitude of RBS signal should be kept as small as possible to keep the system with in the linear region but large enough to excite the process significantly.

By using the process knowledge it is decided that two to five percent change in the input from its steady state value would be enough to get the desired result. Due to small bandwidth of RBS, large simulation time is required to get suitable number of positive and negative step changes. The simulation time for our experiment is chosen 5000 seconds.

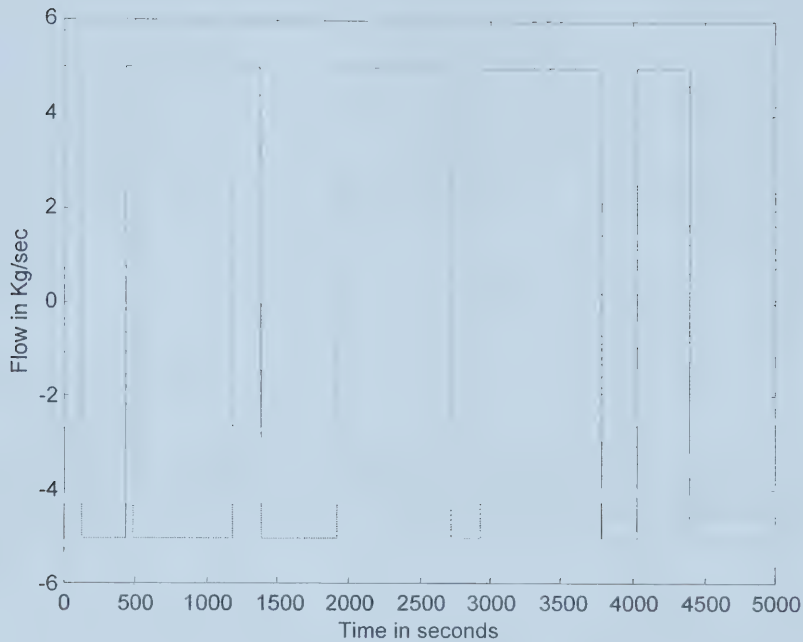


Figure 3.1: Random Binary Signal Applied as Input

3.6 Steady State Operating Points

Models identified using N4SID are linear. In case of a non-linear plant, linear model obtained is only true for certain range of operating conditions. The model obtained at one operating point cannot capture all the dynamics at other operating point. To cover the whole operating range we need to select different steady state operating points and identify model at each point. The operating range for the utility boiler at

Syncrude Utility Plant is between 250 KPPH (44 Kg/sec) and 750 KPPH (94.57 Kg/sec).

The following three operating points are selected:

1. Low Operating Point at steam flow rate of 350 KPPH.
2. Middle Operating Point at steam flow rate of 550 KPPH.
3. High Operating Point at steam flow rate of 700 KPPH.

The process parameters at each operating point are provided in Table A1 as Appendix-A.

3.7 Utility Boiler Models

Three models are identified for Utility Boiler at each selected operating point. For low operating point (LOP), the following **A**, **B**, **C** and **D** matrices represents the state space model:

$$\mathbf{A} = \begin{bmatrix} 0.1320 & -0.2827 & 0.66350 \\ 0.1021 & -0.2099 & 0.46570 \\ 0.0137 & -0.0280 & 0.06080 \end{bmatrix}, \mathbf{B} = \begin{bmatrix} 0.0683 \\ 0.0433 \\ 0.0061 \end{bmatrix}$$

$$\mathbf{C} = [-11.1366 \quad 21.6540 \quad -47.1108], \mathbf{D} = -0.4757$$

Where:

u = Steam Load

y = Drum Pressure

x_1 = Furnace Gas Temperature $-(0.0721)u$

x_2 = Super Heater Gas Temperature $-(0.1344)u$

x_3 = Economizer Gas Temperature $-(0.0464)u$

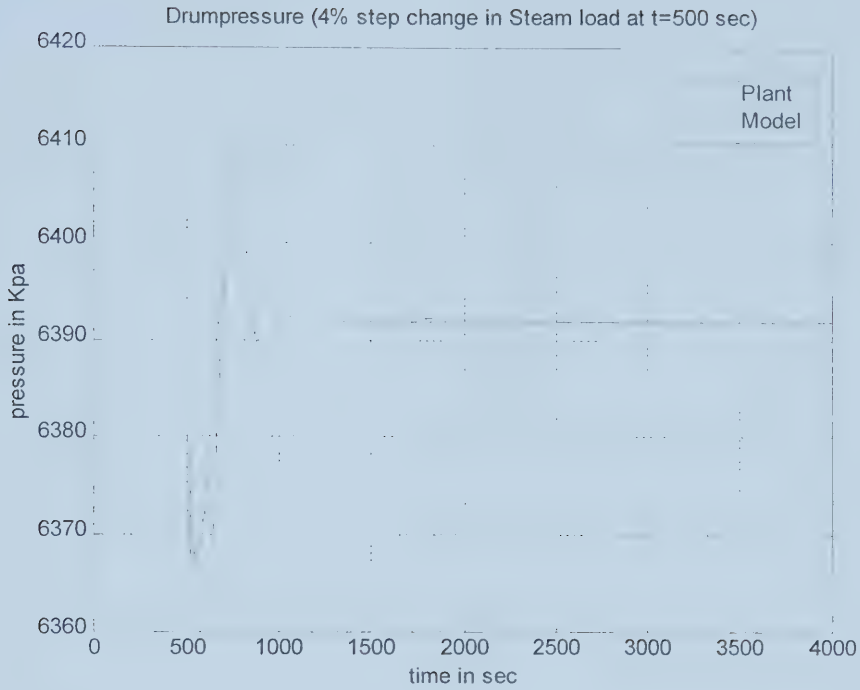


Figure 3.2: Drum Pressure Response to Step Change in Steam Load (LOP)

For middle operating point (MOP) the following are the parameters of state space model:

$$\mathbf{A} = \begin{bmatrix} -0.7927 & 1.2592 & -4.9913 \\ -0.6775 & 1.0806 & -4.3029 \\ -0.0463 & 0.0746 & -0.3015 \end{bmatrix}, \mathbf{B} = \begin{bmatrix} 0.0470 \\ 0.0360 \\ 0.0015 \end{bmatrix},$$

$$\mathbf{C} = [101.6679 \quad -162.7801 \quad 642.5514], \mathbf{D} = -0.5804$$

Where:

u = Steam Load

y = Drum Pressure

x_1 = Furnace Gas Temperature $-(-0.1540)u$

x_2 = Super Heater Gas Temperature $-(-0.0530)u$

x_3 = Economizer Gas Temperature $-(0.2710)u$

For high operating point:

$$\mathbf{A} = \begin{bmatrix} -0.4723 & 0.7708 & -4.8314 \\ -0.4056 & -0.6657 & -4.2173 \\ -0.0190 & 0.0317 & -0.2056 \end{bmatrix}, \mathbf{B} = \begin{bmatrix} 0.0326 \\ 0.0282 \\ 0.0012 \end{bmatrix},$$

$$\mathbf{C} = [99.7865 \quad -160.2198 \quad 937.7032], \mathbf{D} = -0.0349$$

Where:

u = Steam Load

y = Drum Pressure

x_1 = Furnace Gas Temperature $-(0.0269)u$

x_2 = Super Heater Gas Temperature $-(0.0664)u$

x_3 = Economizer Gas Temperature $-(0.0439)u$

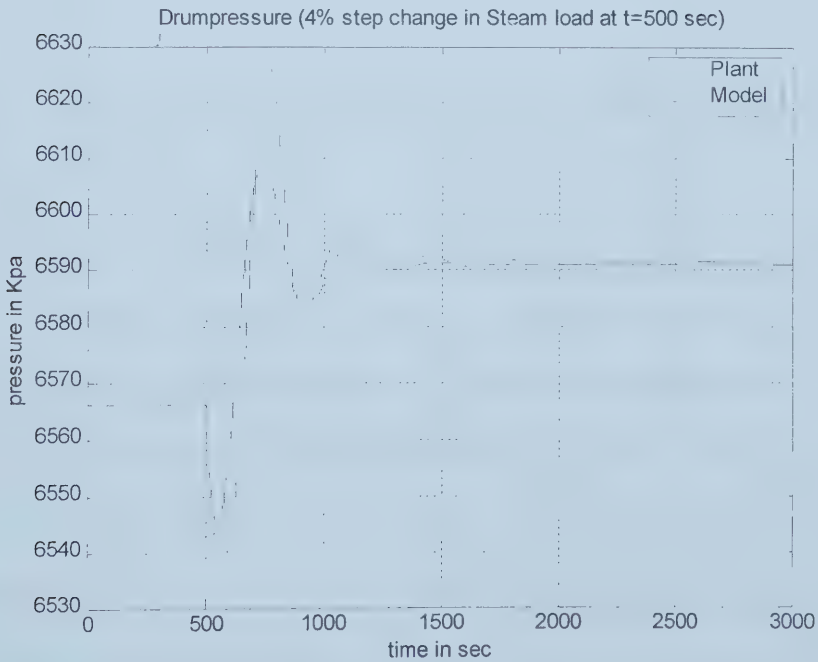


Figure 3.3: Drum Pressure Response to Step Change in Steam Load (MOP)

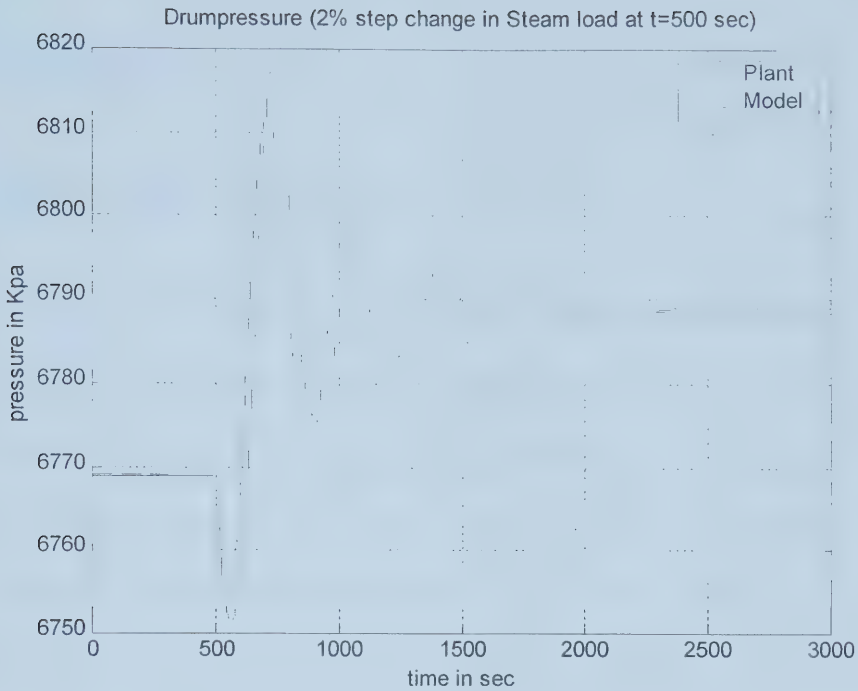


Figure 3.4: Drum Pressure Response to Step Change in Steam Load (HOP)

To validate LOP model, steam load is increased by 4% in step fashion. The output response - pressure change due to change in steam load- of model and the plant are compared. The comparison is shown in figure 3.2 and it can be observed that model is not responding as aggressively as the plant in the first cycle of transient but later on it approximates the plant output quickly. Figure 3.3 and Figure 3.4 give the output response of the model for Middle Operating Point (MOP) and High Operating Point (HOP) respectively. Figure 3.3 shows that model responds to step change similar to the plant. Figure 3.4 shows that we need to add time delay element to match model response to that of the plant. But to keep our calculation simple, we ignore this fact unless we feel that, not incorporating time delay is the major cause of poor design.

Chapter 4

Observer Design

This chapter deals with the design of input-output observer based on H_∞ design methodology to provide a solution to state estimation. The input-output observer approach is applied to the model of large natural circulation gas/oil fired boiler identified in chapter 3. Input-output observer contains a controller in order to minimize an objective function. Observer design is thus transformed into a controller design. H_∞ Controllers are designed for all the three models representing different operating points. The designed controller for each operating point is used as part of the corresponding observer. States estimated by the resultant observer are compared with the actual values given by the plant (SYNSIM in our case). After analyzing simulation results, the benefits, drawbacks and limitations of the proposed observer for this particular application are discussed.

4.1 H_∞ Optimal Control

The shortcomings of LQG motivated the application of H_∞ optimization in robust control. This trend was set by influential work of Zames [21]. He also criticized the representation of uncertain disturbances by white noise process. Later Glover and Doyle [22] and Doyle et al. [23] contributed significantly by providing the solution in state space domain.

For any system \mathbf{P} with input vector \mathbf{w} and output vector \mathbf{v} , the H_∞ norm of \mathbf{P} is defined as:

$$\|\hat{p}\|_\infty = \sup_{\omega} \sigma_{\max} [\hat{p}(j\omega)] \quad (4.1)$$

Where $\hat{p}(s)$ is a complex function of order $m \times n$, m being the dimension of system output vector and n the dimension of system input vector. $\sigma_{\max} [\hat{p}(j\omega)]$ denotes the maximum singular value of $\hat{p}(j\omega)$. H_∞ norm is also equal to the system gain i.e. maximum L_2 norm of the output over all inputs of unit norm. This can be expressed mathematically as:

$$\|\hat{p}\|_\infty = \sup \{ \|v\|_2 : \|w\|_2 = 1 \} \quad (4.2)$$

There are many ways in which the feedback design problem can be cast as H_∞ optimization problem. It is therefore useful to have standard formulation in which a particular problem may be manipulated. Such a general formulation is afforded by the general configuration shown in figure 4.1.

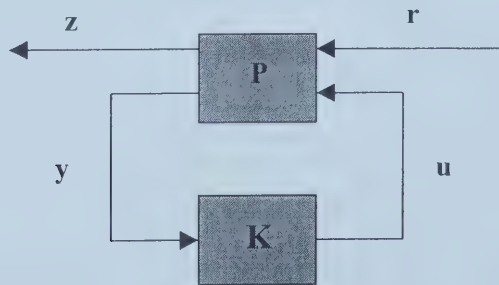


Figure 4.1: Standard H_∞ formulation

Here \mathbf{r} , \mathbf{u} , \mathbf{y} and \mathbf{z} are continuous time signals whose magnitudes can be any real numbers, and \mathbf{P} and \mathbf{K} are the generalized plant and the controller respectively. Vector \mathbf{r} represents exogenous inputs to the plant including the reference command, disturbance and sensor noise; vector \mathbf{u} represents the plant inputs (controller outputs); vector \mathbf{y} represents measured signals (controller inputs); and vector \mathbf{z} represents signals to be controlled.

Consider the generalized system in figure 4.1, and let the closed loop system from \mathbf{r} to \mathbf{z} be denoted by \mathbf{P}_{zr} with transfer function matrix $\hat{p}_{zr}(s)$. The H_∞ problem is in fact the problem to find an internally stabilizing controller \mathbf{K} based on the information \mathbf{y} , which generates \mathbf{u} to counteract the influence of \mathbf{r} on \mathbf{z} , thereby minimizing the closed loop norm $\|\hat{p}_{zr}\|_\infty$. The most important point here to appreciate is that almost any linear control problem can be formulated using block diagram in figure 4.1. The configuration may at first glance seem restrictive, however, this is not the case. The generality of the set up can be extended to the design of observers as well as feedforward controllers. The routines in MATLAB for synthesizing H_∞ controllers assume that the problem is in general form i.e. \mathbf{P} is given. To construct \mathbf{P} it should be kept in mind that it is an open loop system and one should break all loops entering and exiting controller \mathbf{K} . Calculation of finding a generalized plant may seem a tedious job but it can be done easily by using MATLAB μ -toolbox command “sysic”. To get a meaningful synthesis problem we generally have to include weights \mathbf{W}_z and \mathbf{W}_r in the generalized plant \mathbf{P} as shown in figure 4.2. That is why we consider the weighted or normalized exogenous inputs \mathbf{r} (where $\mathbf{r} = \mathbf{W}_r \mathbf{r}$) and the weighted or normalized output \mathbf{z} (where $\mathbf{z} = \mathbf{W}_z \mathbf{z}$).

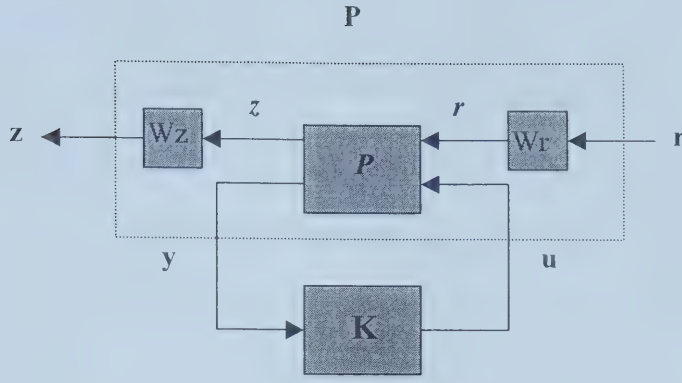


Figure 4.2: General H_∞ formulation with Weightings

The generalized plant **P** has four types of external variables; **z**, **y**, **r** and **u**. They are correlated through the linear state space equation:

$$\mathbf{P} = \left\langle \begin{array}{c|c} \mathbf{A} & \mathbf{B} \\ \hline \mathbf{C} & \mathbf{D} \end{array} \right\rangle \quad (4.3)$$

Because the input & output of **P** are partitioned as $\begin{pmatrix} \mathbf{r} \\ \mathbf{u} \end{pmatrix}$ and $\begin{pmatrix} \mathbf{z} \\ \mathbf{y} \end{pmatrix}$, we have

$$\mathbf{G} = \left\langle \begin{array}{c|cc} \mathbf{A} & \mathbf{B}_1 & \mathbf{B}_2 \\ \hline \mathbf{C}_1 & \mathbf{D}_{11} & \mathbf{D}_{12} \\ \mathbf{C}_2 & \mathbf{D}_{21} & \mathbf{D}_{22} \end{array} \right\rangle \quad (4.4)$$

The following requirements need to be checked about the open loop system **P** to guarantee the existence of an optimal controller **K**:

1. $(\mathbf{A}, \mathbf{B}_2)$ is stabilizable and $(\mathbf{C}_2, \mathbf{A})$ is detectable.
2. \mathbf{D}_{12} has full column rank and \mathbf{D}_{21} has full row rank.
3. $\begin{pmatrix} \mathbf{A} - j\omega\mathbf{I} & \mathbf{B}_2 \\ \mathbf{C}_1 & \mathbf{D}_{12} \end{pmatrix}$ has full column rank for all ω , and $\begin{pmatrix} \mathbf{A} - j\omega\mathbf{I} & \mathbf{B}_1 \\ \mathbf{C}_2 & \mathbf{D}_{21} \end{pmatrix}$ has full row rank for all ω .

4. $\mathbf{D}_{11}=0$ and $\mathbf{D}_{22}=0$.

Condition (1) is required for the existence of stabilizing controller \mathbf{K} while condition (2) is required to ensure that the controller is proper and hence realizable. Condition (3) ensures that the optimal controller does not try to cancel poles or zeros on the imaginary axis, which would result in closed loop instability. Condition (4) is really not required but it would simplify the problem. If \mathbf{D}_{11} and \mathbf{D}_{22} are not zero, an equivalent H_∞ problem can be constructed in which they are; see Safanov et al. [24] and Green and Limbeer [25]. While the above conditions may appear daunting, most sensibly posed control problems will meet them. It is worth to note that it is hard to get an optimal controller so the problem is reduced to finding a sub-optimal controller. For a specified γ a stabilizing sub-optimal controller is found for which the infinity norm of the $\|F_l(\mathbf{P}, \mathbf{K})\|_\infty < \gamma$, where F_l stands for Linear Fractional Transformation. The algorithm can be used iteratively, reducing γ until minimum is reached.

If all the requirements are satisfied then the problem can be solved efficiently by using the algorithm of Doyle et al. [23].

4.2 H_∞ Loop shaping design method

This method is based on the combination of H_∞ robust stabilization and classical loop shaping as proposed by Mcfarlane and Glover [26, 28]. It is a two-stage design process. In the first stage, open loop plant is augmented by pre and post compensators, in order to shape the singular values of the open loop frequency response. In the second stage, the resulting shaped plant is robustly stabilized with

respect to co-prime factor uncertainty using H_∞ optimization. The advantage with this method is that no weight selection or modeling of problem-dependent uncertainty is required and also it does not require γ -iteration for its solution. The step by step procedure for H_∞ loop-shaping design is presented below which is taken from Skogestad and Postlethwaite [11]. This procedure has its origin in the PhD thesis by Hyde [27] and since been successfully applied to several industrial problems. In fact it is a single degree-of-freedom controller and this can be a limitation if there are stringent requirements on command following.

The step by step procedure is as follows (taken from [11]):

1. Scale the plant outputs and inputs. It improves the conditioning of the design problem, enables meaningful analysis of the robustness properties of the feedback system in the frequency domain. Also for loop shaping it can simplify the selection of weights. Scaling with respect to maximum values is one of the several options.
2. Order inputs and outputs so that the plant is as diagonal as possible. The relative gain array can be useful. This will make the design of pre and post compensators easy which, for simplicity, will be chosen to be diagonal.
3. Select suitable weights \mathbf{W}_1 and \mathbf{W}_2 to obtain the shaped plant $\mathbf{P}_s = \mathbf{W}_2 \mathbf{P} \mathbf{W}_1$. \mathbf{W}_1 is called pre compensator and \mathbf{W}_2 post compensator. Selection should be made in a such a way so that the singular values of \mathbf{P}_s are shaped as desirable. This would normally mean high gain at low frequencies, roll-off rates of approximately 20db/decade (a slope of about -1) at the desired bandwidth, with higher rates at high frequencies. Some trial and error is involved here. \mathbf{W}_2 is usually chosen as

constant, reflecting the relative importance of the outputs to be controlled and other measurements being fed back to the controller. \mathbf{W}_1 contains the dynamic shaping. Integral action, for low frequency performance; phase-advance for reducing the roll-off rates at cross over; and phase-lag to increase the roll-off rates at higher frequencies should all be placed in \mathbf{W}_1 if desired. The weights should be chosen so that no unstable hidden modes are created in \mathbf{P}_s .

4. Robustly stabilize the shaped plant \mathbf{P}_s . First calculate the maximum stability margin $\epsilon_{\max} = 1/\gamma_{\min}$. If the margin is too small, $\epsilon_{\max} < 0.25$, then go back to step 3 and modify the weights. Otherwise select $\gamma > \gamma_{\min}$, by about 10% and synthesize a sub-optimal controller. This function gives a controller \mathbf{K}_s for the shaped plant \mathbf{P}_s . The feedback controller for plant \mathbf{P} is then \mathbf{K} where $\mathbf{K} = \mathbf{W}_1 \mathbf{K}_s \mathbf{W}_2$. It is important here to emphasize that since, we can compute γ_{\min} , we can get an explicit solution by solving just two Riccati equations and can avoid the γ iteration needed to solve general H_∞ problem.
5. Analyze the design and if all the specifications are not met, make further modifications to the weights.
6. Implement the control after getting satisfactory performance.

Some of the advantages offered by H_∞ loop-shaping design procedure are:

1. It is relatively easy to use, being based on classical loop shaping ideas.
2. There exist a closed formula for the H_∞ optimal cost γ_{\min} which in turn corresponds to maximum stability margin $\epsilon_{\max} = 1/\gamma_{\min}$.
3. No γ -iteration is involved in the solution.

4. Except for special systems, one with all pass factors, there are no pole-zero cancellation between the plant and the controller. Pole-zero cancellations are very common in H_∞ control problems and create troubles when the plant has lightly damped modes.

4.3 Controller Model Order Reduction

Modern controller design methods, such as H_∞ and LQG, produce controller of the order at least equal to that of the plant, and usually higher because of the inclusion of weights. These control laws may be too complex to implement and therefore simpler designs are then sought. Several approaches can be taken i.e. to reduce the order of the plant model prior to controller design, or reduce the controller in later stage, or both. In our case the controllers are first designed and then reduced.

There are three methods to reduce the order of a controller model: balanced truncation, balanced residualization and optimal Hankel norm approximation. Each method gives a stable approximation and a guaranteed bound on the error. All these methods are based on a special state space realization of \mathbf{K} referred to as balanced realization. Residualization unlike truncation and optimal Hankel norm approximation, preserve the steady state gain of the system, and, like truncation, it is simple and computationally inexpensive. Skogestad and Postlethwaite [11] states that truncation and optimal Hankel norm approximation perform better at high frequencies, where as residualization performs better at low and medium frequencies, i.e. up to the critical frequencies. Thus for the plant model reduction, where models are not accurate at high frequencies to start with, residualization seems to be better

choice. Further if steady state gains are to be kept unchanged, truncated or Hankel norm approximated systems require scaling, which may result in large errors. In such a case, too, residualization would be preferred choice.

In frequency weighted model reduction method, the idea is to emphasize frequency ranges where better matching is required. This, however, has been observed to have effect of producing larger errors at other frequencies. In order to get good steady state matching, a relatively large weight would have to be used at steady state, which would cause poorer matching elsewhere. The choice of weight is not straight forward, and an error bound is available only for weighted Hankel norm approximation. The computation of bound is not as easy as in the unweighted case. Balanced residualization in this context is seen as a reduction scheme with implicit low and medium frequency weighting.

In general steady state gain matching may not be crucial, but the matching should usually be good near the desired closed loop bandwidth. Balanced residualization has been seen to perform close to the full order system in this frequency range. Good approximation at high frequencies may also some times be desired. In such a case, using truncation or optimal Hankel norm approximation with appropriate frequency weightings may yield better results.

4.4 Observer Design

As discussed in chapter 2, if \mathbf{G} is an internally stabilizing controller and the error between estimated and actual output is minimized then the estimated state would asymptotically track the actual state. This is the same property as exhibits by

Luenberger Observer. An important point to note is that our model, representing Syncrude utility boiler, has one input, and three states and it is not possible to guarantee the minimum possible state error for all frequencies. However, it is possible to design an internally stabilizing controller that minimizes the infinity norm of an output error signal in order to guarantee asymptotic tracking of estimated states to that of actual states. This approach would be followed in the observer design given in this chapter.

Our objective here is to design three observers for three different operating ranges using their respective boiler models. The three reference operating points (as discussed in chapter 3) are:

1. High Operating Point –HOP (Steam Load = 249.7 Kg/sec)
2. Middle Operating Point –MOP (Steam Load = 192.9 Kg/sec)
3. Low Operating Point –LOP (Steam Load = 117.2 Kg/sec)

4.4.1 Observer Design for HOP

Suitable weights \mathbf{W}_1 and \mathbf{W}_2 are selected to obtain the shaped plant $\mathbf{P}_s = \mathbf{W}_2 \mathbf{P} \mathbf{W}_1$. \mathbf{W}_1 is called pre-compensator and \mathbf{W}_2 post-compensator. Selection is made in such a way so that singular values of \mathbf{P}_s are shaped as desired. Maximum singular value is some times very useful in terms of frequency domain performance and robustness. It gives useful information about the effectiveness of the feedback control. For asymptotic tracking the maximum singular value of sensitivity function $[\mathbf{I} + \mathbf{C}\mathbf{F}_0\mathbf{G}]^{-1}$ should be small at low frequencies where the feedback control is effective while it approaches 1 at high frequencies because any real system is strictly proper. The

maximum singular value would have peak at around crossover frequency. This peak is undesirable but unavoidable for real systems. Because our system is SISO, we do not need to emphasize the relative importance of the outputs to be controlled and other measurements being fed back to the controller. Therefore \mathbf{W}_2 in our case is chosen as constant 1. \mathbf{W}_1 contains the dynamic shaping i.e. integral action, for low frequency performance; phase-advance for reducing the roll-off rates at cross over; and phase-lag to increase the roll-off rates at higher frequencies.

We are interested in shaping the magnitude of transfer function $|\mathbf{P}_s(j\omega)|$. Essentially to get the benefits of feedback control we want the loop gain, $\mathbf{L}(s) = \mathbf{P}_s(s)\mathbf{G}(s)$, to be as large as possible with in the bandwidth region. However due to RHP-zero, the loop gain $\mathbf{L}(s)$ has to drop below one at above some frequency, which we call critical frequency. It is desirable that $|\mathbf{P}_s(j\omega)|$ falls sharply with frequency. To measure the slope of $|\mathbf{P}_s(j\omega)|$ logarithmic slope $N = d\ln|\mathbf{P}_s|/d\ln\omega$ is used. For example the slope of $N = -1$ implies that $|\mathbf{P}_s|$ drops by a factor of 10 when ω increases by factor of 10. In our case the gain is measured in decibels (dB), therefore $N = -1$ means a change of -20dB/decade . The value of $-N$ at high frequencies is called roll-off rate. The desired shape for $|\mathbf{P}_s(j\omega)|$ should have a slope of about -1 in the crossover region, and slope of -2 or higher beyond this frequency, that is roll-off is 2 or larger. Because we are considering step changes in the reference/disturbance, which affects outputs in steps, a slope of -1 is acceptable.

In practice, integrators are included in the controller to get the desired low-frequency performance. Therefore in selecting our weightings for \mathbf{W}_1 we include at least one

integrator to \mathbf{W}_1 . This ensures that loop gain $\mathbf{L}(s) = \mathbf{P}_s(s)\mathbf{G}(s)$ will contain at least one integrator and will provide offset free reference tracking.

Case-I

Some trial and error is always involved in choosing \mathbf{W}_1 . The following weighting is taken as a starting point:

$$\mathbf{W}_1 = \frac{0.001}{s} \quad (4.1)$$

This trial is labeled as Case-I. The singular value of shaped plant $\mathbf{W}_2 \mathbf{P} \mathbf{W}_1$ for Case-I is given in figure 4.3.

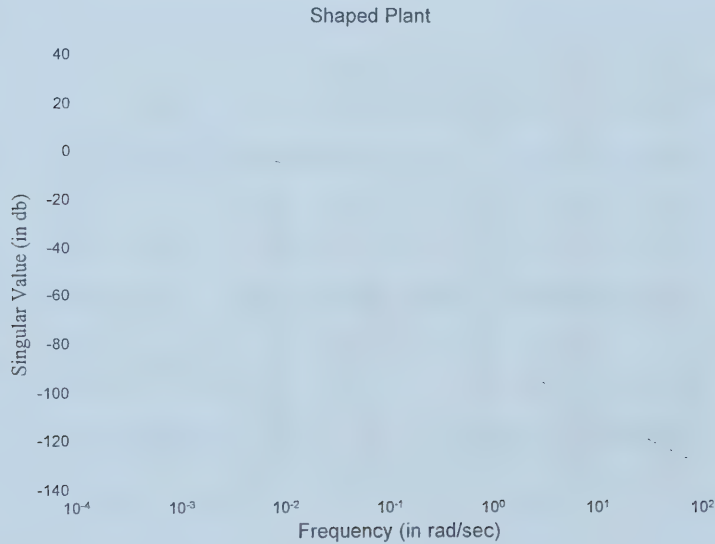


Figure 4.3: Shaped Plant for Case-I

From chapter 3, it is known that the boiler model for HOP has one zero in positive real half-plane. This positive real half-plane zero exhibits the inverse response characteristics of the boiler and is due to the shrink and swell effect. The location of

this zero is at $s=0.0126$ and its effect can be seen in figure 4.3. The slope of the shaped plant is -1 at frequencies lower than $\omega=0.0126$ rad/sec while it is almost -2 at frequencies higher than $\omega=0.0126$ rad/sec. But there is a significant bump at $\omega=0.0126$ rad./sec. which has resulted in a poor shaping of the plant. Several other weightings of the same kind are tried but to get desired slope at around the RHP zero is not achieved. A different approach towards the selection of weighting functions needs to be adopted in order to overcome this difficulty (which is discussed as Case-II). However, before applying that approach we are interested in the design of the observer for Case-I to observe the limitation imposed in the presence of RHP-zero.

Using \mathbf{W}_1 from eq.(4.1), an \mathbf{H}_∞ controller $\mathbf{G1}_c$ was designed according to method described in §4.2. The resultant controller has an order of four (see appendix B). The desired controller should ensure stability as well as provide good tracking properties. Stability is not an issue here because the \mathbf{H}_∞ algorithm used to design the controller automatically takes care of the stability factor. The best means to analyze the performance of the controller would be to look into singular value plot of sensitivity function and step response curve of the closed loop transfer function.

Figure 4.4 shows that at around $\omega=0.0126$, the location of RHP-zero, there is a significant amount of fluctuation. The controller would behave in a strange manner at frequencies within the range around $\omega=0.0126$. Our immediate concern is to remove this fluctuation by partially neutralizing the effect of RHP-zero while choosing weighting function \mathbf{W}_1 .

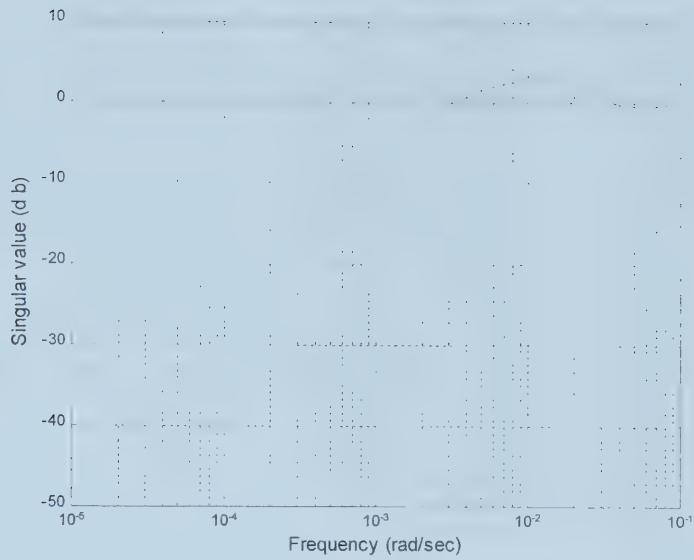


Figure 4.4: Singular Value Plot of Sensitivity Function (HOP :Case-I)

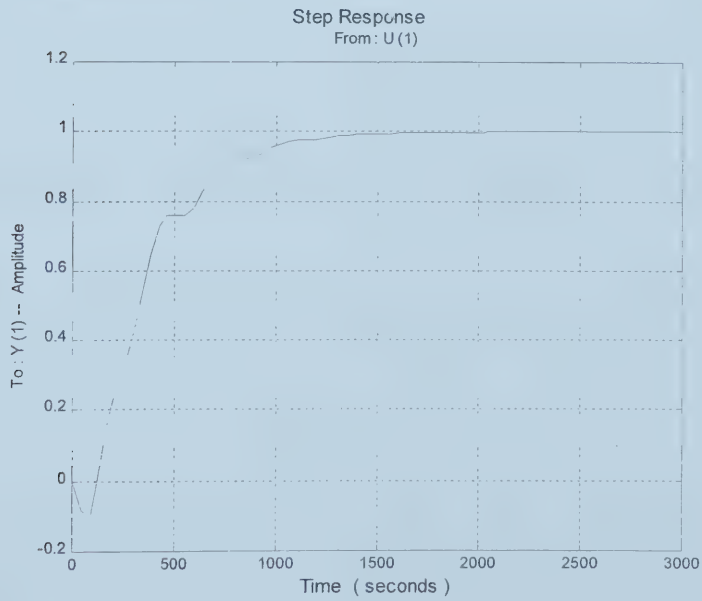


Figure 4.5: Output Step Response using controller $G1_c$ (HOP :Case-I)

The general criterion about the performance in the presence of RHP-zero z requires that the crossover frequency ω_c should be less than z . This is a serious limitation imposed by RHP-zero. Crossover frequency ω_c in this case is 0.00125. Good tracking properties are exhibited in the low frequency range up to $\omega=0.0005$, where the singular value is well below -10 dB. As the Bandwidth ω_B is always less than ω_c , in this case the bandwidth is very small which eventually would affect the speed of output response. The slow speed of output response can be observed from figure 4.5.

Case-II

To reduce the effect of RHP-zero we need to choose a suitable value for \mathbf{W}_1 . We have RHP zero at $z = 0.0126$. RHP zero limits the achievable bandwidth and so the cross over limit cannot exceed $\omega = 0.0126$.

We require the system to have an integrator and the reasonable approach is to let the shaped plant transfer function have a slope of -1 at low frequencies and then to roll off with a higher slope at frequencies beyond 0.0126 rad/sec. Our choice of weight \mathbf{W}_1 will be:

$$\mathbf{W}_1 = 0.1 \left[\frac{(s - 0.0024 + 0.0193j)(s - 0.0024 - 0.0193j)}{s(s + 0.0126)} \right] \quad (4.2)$$

The controller should have zeros at the locations of plant poles because we do not want the slope of loop shape to drop just before crossover. To avoid an increase in slope caused by the zero we place a pole $s = -0.0126$ such that the loop transfer

function contains the term $(-s + z)/(s + z)$, the form of which is referred to as all pass since its magnitude equals 1 at all frequencies.

The HOP model has poles at:

$$s = -0.0024 + 0.0193j, -0.0024 - 0.0193j, -0.0074$$

And zeros at:

$$s = -3.4239, -0.0072, +0.0126$$

Therefore the term $(s - 0.0024 + 0.0193j)(s - 0.0024 - 0.0193j)$ is included in the numerator and the term $(s + 0.0126)$ is included in the denominator of \mathbf{W}_1 .

Figure 4.6 shows the singular value plot of the shaped plant \mathbf{P}_s . By comparing it with the shaped plant in case-I, it can be observed that the bump in the curve at RHP-zero location has been almost eliminated. The slope of the curve is between -1 and -2 before $\omega = 1$ rad/sec while it becomes zero after $\omega = 10$ rad/sec.

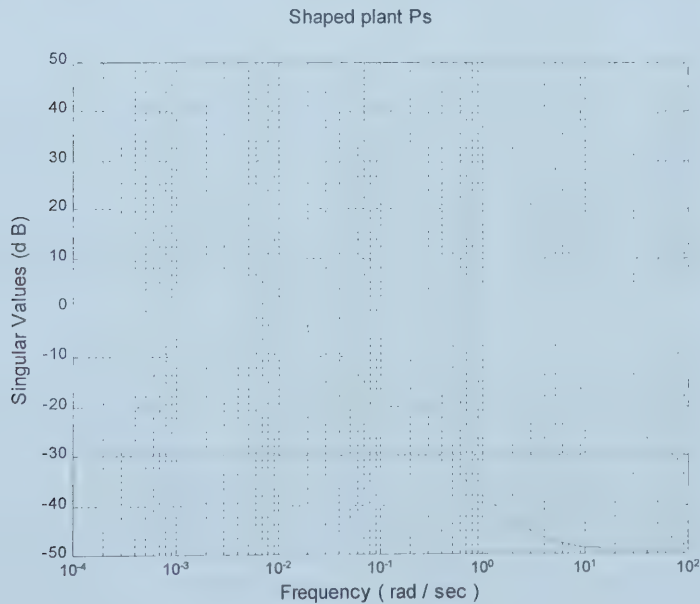


Figure 4.6: Shaped Plant \mathbf{P}_s (HOP : Case-II)

The design method explained in §4.2 is used with new weightings \mathbf{W}_1 and a sixth order controller $\mathbf{G1}$ is obtained (see Appendix-B). The singular value plot for the sensitivity function $[\mathbf{I}+\mathbf{CF}_0\mathbf{G}]^{-1}$ is shown in figure 4.7. It can be seen that there is no bump at and around $\omega=0.0126$ rad/sec, the RHP-zero location as was in the previous case. The transition from peak value back to zero is smooth and as desired. Another improvement can be seen in the location of the crossover frequency, which is moved towards right from 0.00125 rad/sec to 0.0015 rad/sec. This would increase the bandwidth and speedup the output response. The negative consequence of moving crossover frequency to right in the presence of RHP-zero is increase in the peak of the curve. This is called waterbed effect. It says that if we push sensitivity function down at some frequencies then it will have to increase at others. The effect is similar to sitting on a waterbed. Pushing it down at one point, which reduces the water level locally will result in increased level some where else on the bed. A trade off between sensitivity reduction and sensitivity increase must be performed whenever $\mathbf{L}(s)$ has RHP-zero. The requirement is to keep sensitivity function as close as zero beyond crossover frequency. But due to limitation by RHP-zero, we have to compromise between the speed of response and the effectiveness of tracking properties.

Step response using $\mathbf{G1}$ is shown in figure 4.8. The rise time in this case is approximately 300 seconds, which is compatible with the process time constant. This controller exhibits faster response than the previous case. Another improvement is the larger negative peak, to approximate the negative response characteristics of the output.

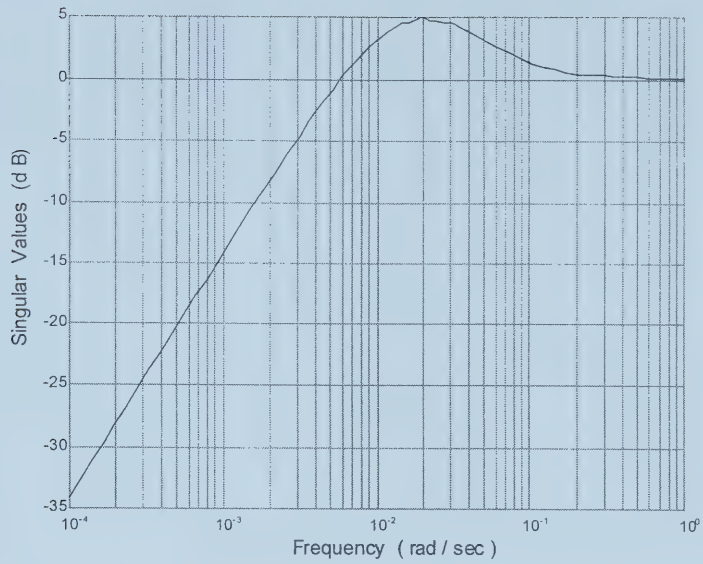


Figure 4.7: Singular Value Plot of Sensitivity Function using G1 (HOP Case-II)

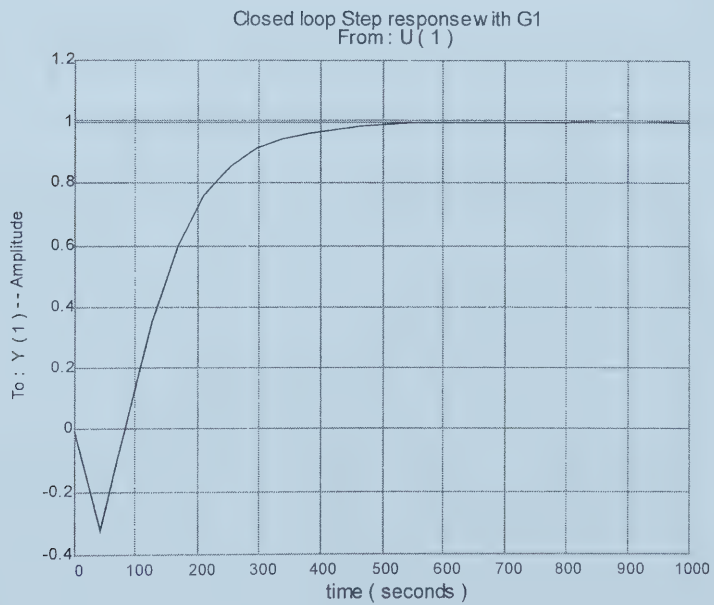


Figure 4.8: Output Step Response using controller G1 (HOP :Case-II)

The only drawback is the poor tracking at frequencies more than 0.001 rad/sec. But because we are interested in steady state tracking, we are ready to compromise on a little bit poor high frequency tracking for fast output response with better inverse response characteristics.

Most of the controllers designed using H_∞ and LQG design techniques, produce controller of the order at least equal to that of the plant, and usually higher because of the inclusion of weights. These control laws are usually too complex to implement. In our case we have tried to reduce the controller order without affecting the overall performance of the controller. The controller order is reduced using methods mentioned in § 4.3.

There are three methods to reduce the order of a controller model: balanced truncation, balanced residualization and optimal Hankel norm approximation. Each method gives a stable approximation and a guaranteed bound on the error. All these methods are based on a special state space realization of $\mathbf{G1}$ referred to as balanced realization. We found that in our case Residualization and Hankel norm approximation performs better than truncation. Reduced order controllers are denoted with letter representing the original controller along with the subscript. The subscript shows the method by which the reduction is performed. Subscript 'r' represents "Balanced Residualization" while subscript 'h' represents "Hankel Norm Approximation".

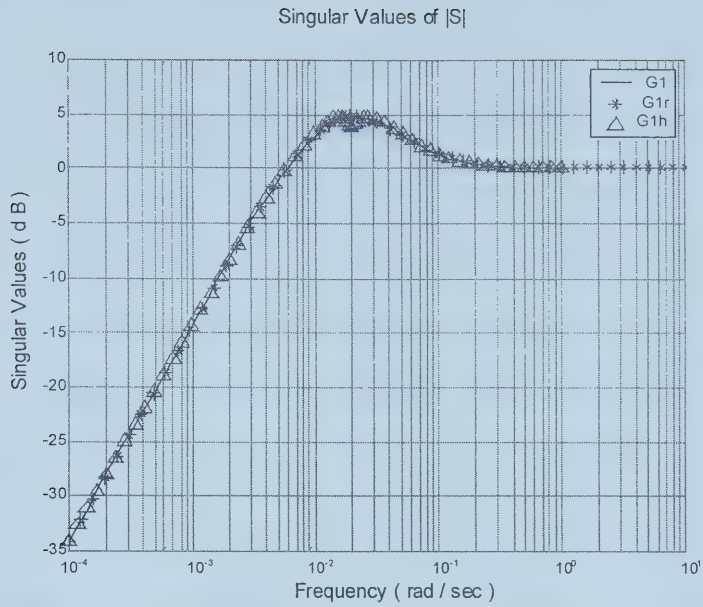


Figure 4.9 : Singular value plot for $|S|$ with controller $G1$, $G1_r$, and $G1_h$

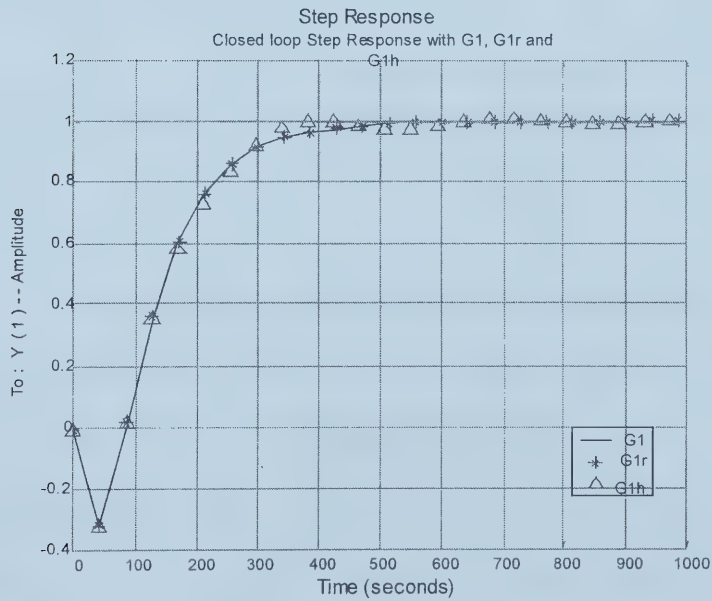


Figure 4.10: Step response with controller $G1$, $G1_r$, and $G1_h$

Figure 4.9 shows the comparison between singular value plots of sensitivity function, using original controller $\mathbf{G1}$ and reduced order controllers $\mathbf{G1}_h$ and $\mathbf{G1}_r$. Similarly, figure 4.10 shows the comparison between the step responses with original controller $\mathbf{G1}$ and reduced order controllers $\mathbf{G1}_h$ and $\mathbf{G1}_r$. $\mathbf{G1}_r$ is the balanced residualization while $\mathbf{G1}_h$ is the Hankel-norm approximation of $\mathbf{G1}$. $\mathbf{G1}$, $\mathbf{G1}_h$ and $\mathbf{G1}_r$ have orders of six, two and four respectively. The step response and singular value plots show that all the three controllers give the same level of performance. And therefore being a low order controller we have selected $\mathbf{G1}_h$ as our controller $\mathbf{G}(s)$ for “Observer 1” (see figure 2.3). Observer 1 is the observer for high operating point HOP. Referring back to chapter 3, it should be noted that the state vector \mathbf{Z} of the model HOP is the difference of vector \mathbf{Y}_{13} and $\mathbf{D}_{13}\mathbf{u}$. Because we are interested in estimation of physical quantities of the boiler that are elements of \mathbf{Y}_{13} , it is calculated by adding $\mathbf{D}_{13}\mathbf{u}$ with \mathbf{Z} during simulation. Recall from chapter 3 that:

$$\mathbf{Y}_{13} = \begin{bmatrix} \mathbf{Y}_1 \\ \mathbf{Y}_2 \\ \mathbf{Y}_3 \end{bmatrix} = \begin{bmatrix} \text{Furnace gas temperature} \\ \text{Superheater gas temperature} \\ \text{Economizer gas temperature} \end{bmatrix}$$

Steam load is changed by 4% in a step fashion from its steady state value of 249.7 kg/sec to 259.69 kg/sec at $t = 500$ seconds. Total time of 4000 seconds is selected for simulation. This is due to the slow dynamics of the process, which takes longer time to come back to steady state. Step change is applied simultaneously to SYNSIM boiler block as well as the Observer block and the estimated parameters given by the observer are compared with actual values given by SYNSIM non-linear model. The simulation results for “Observer 1” using model HOP and controller $\mathbf{G1}_h$ are shown in

figure 4.11, figure 4.12 and figure 4.13. It can be observed from these results that the estimated states track the actual state asymptotically. After the change is applied, the first cycle of the estimated state does not match with the first cycle of the actual state for all the three plots. This due to the poor tracking properties at high frequencies; a limitation imposed by RHP-zero. At low frequencies the observer is performing well as its estimated states perfectly tracks actual states at steady state. In case of economizer gas temperature, the actual values plot exhibits some sort of non-linearity and the observer is trying to approximate the non-linear characteristic in the best possible way so as get faster steady state tracking.

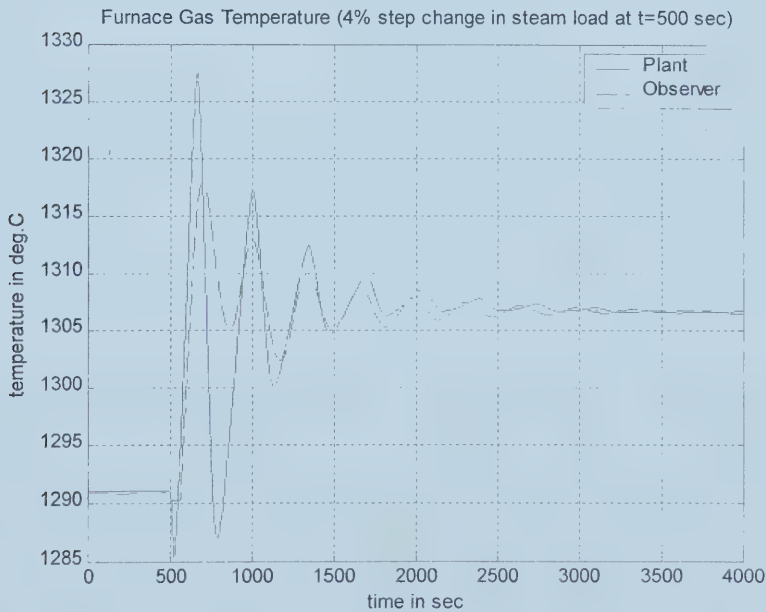


Figure 4.11: Estimated vs. Actual Furnace Gas Temperature (HOP)

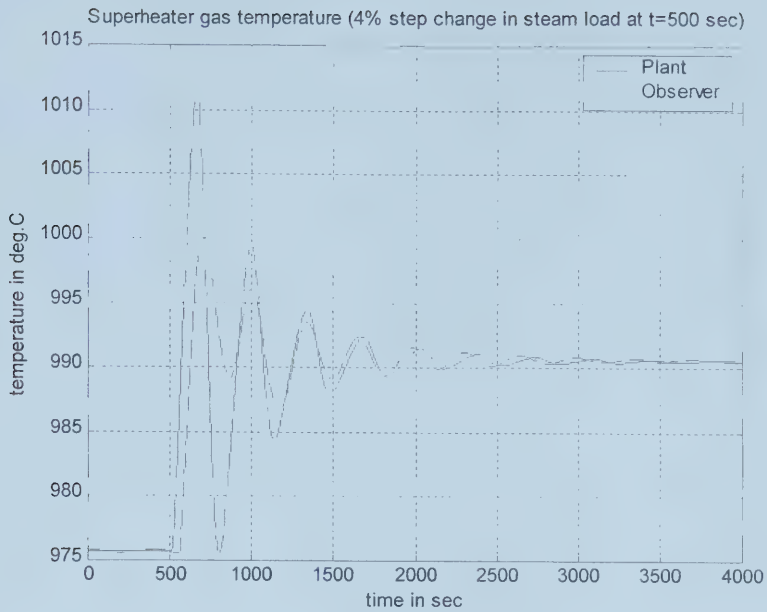


Figure 4.12: Estimated vs. Actual Super-heater Gas Temperature (HOP)

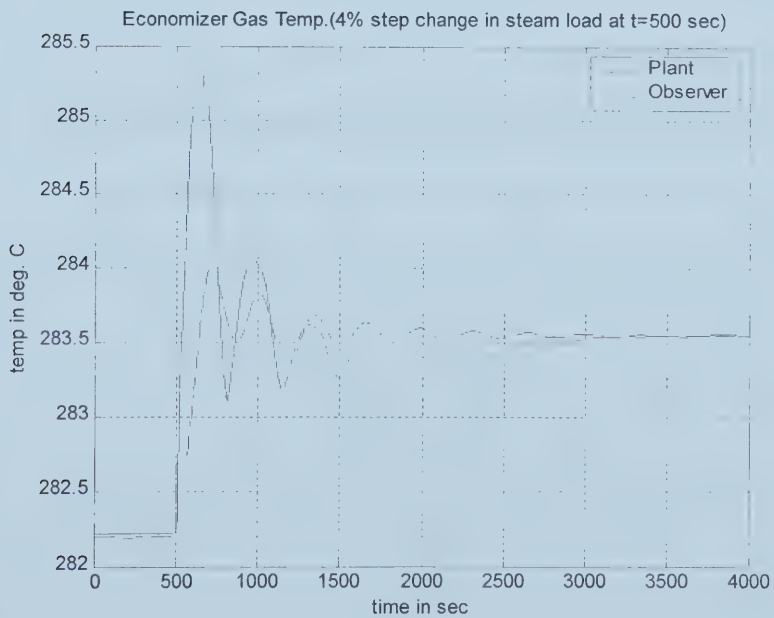


Figure 4.13: Estimated vs. Actual Economizer Gas Temperature (HOP)

4.4.2 Observer Design for MOP

The design procedure for Middle Operating Point (MOP) is exactly the repetition of the design procedure for High Operating Point (HOP). The model for MOP has one real and a pair of complex poles. The pair of complex poles lies at $s = -0.0046 \pm 0.017j$. Out of three zeros in total, one zero lies at $s = +0.0091$ which is right half plane zero. By taking into consideration these poles and zeros of the plant model MOP, our choice for weight function \mathbf{W}_1 is:

$$\mathbf{W}_1 = 0.1 \left[\frac{(s + 0.0046 - 0.017j)(s + 0.0046 + 0.017j)}{s(s + 0.0091)} \right]$$

Singular values of the shaped plant \mathbf{P}_s are shown in figure 4.14. A sixth order Controller $\mathbf{G2}$ is obtained. The singular value plot of a sensitivity function, using controller $\mathbf{G2}$, is shown in figure 4.15. $\mathbf{G2}$ being high order controller is reduced through Hankel norm approximation technique to a second order controller $\mathbf{G2}_h$. The closed loop step response comparison and singular value plot comparison of sensitivity function for original controller $\mathbf{G2}$ and reduced order controller $\mathbf{G2}_h$ are given in figure 4.16 and figure 4.17 respectively. It can be observed from these results that the performance given by $\mathbf{G2}_h$ is the same as $\mathbf{G2}$. $\mathbf{G2}_h$ being a low order controller is selected as controller $\mathbf{G}(s)$ for our “Observer 2” (see figure 2.3). “Observer 2” is the observer designed for Middle Operating Point.

A 4% change is applied at $t = 500$ seconds to SYNSIM boiler model and “Observer 2” simultaneously. Steam load is changed from steady state value of 192.9 kg/sec to 200.61 kg/sec. States estimated by the observer are compared with the actual states given by SYNSIM model, assumed as plant. The comparison is given in figure 4.18, figure 4.19 and figure 4.20.

It can be concluded from the above results that although tracking is poor at high frequencies, the estimated states approximate the actual states at low frequencies and the observer performance is good enough for asymptotic tracking of actual states.

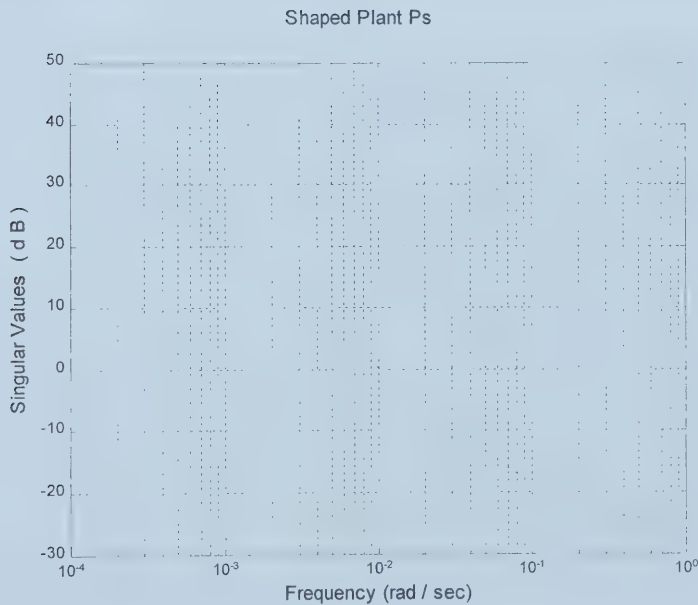


Figure 4.14: Shaped Plant P_s (MOP)

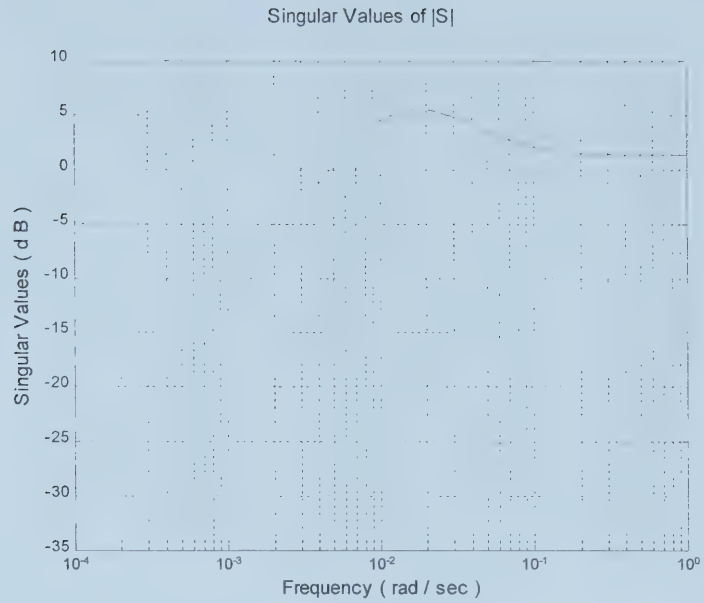


Figure 4.15: Singular Value Plot for $|S|$ using controller G2 (MOP)

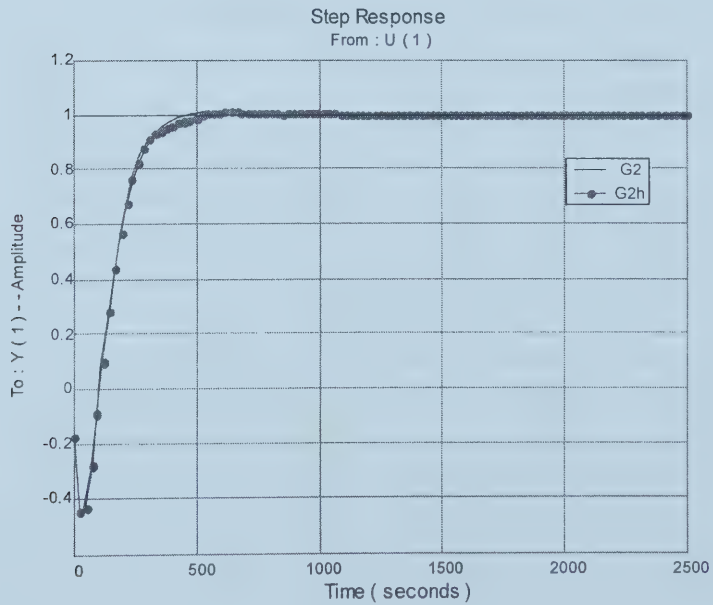


Figure 4.16: Output Step Response using controller G2 and G2_h (MOP)

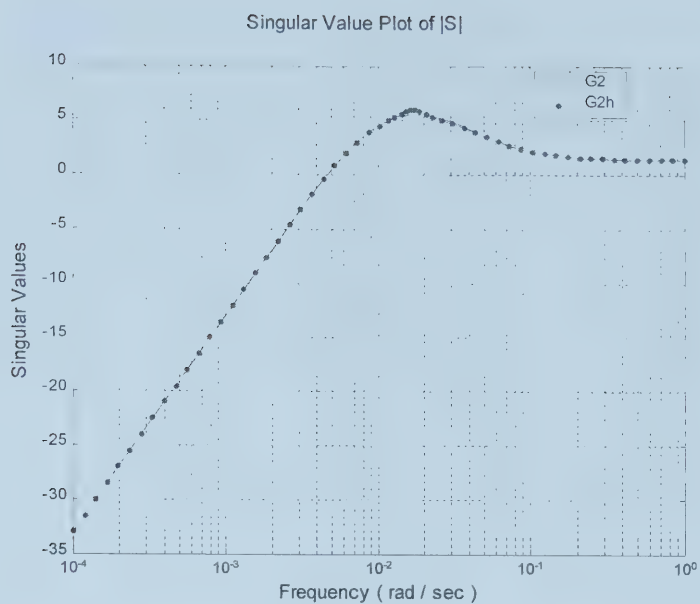


Figure 4.17: Singular value plot for $|S|$ with controller G2 and G2_h (MOP)

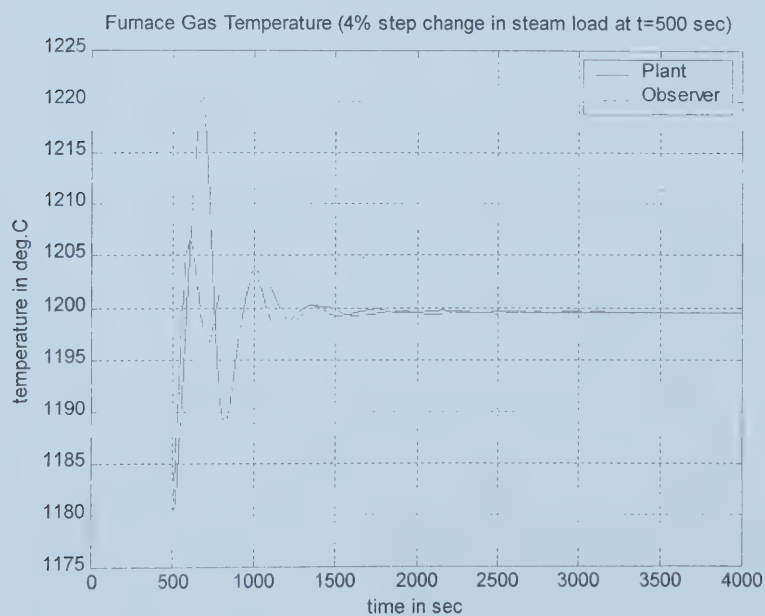


Figure 4.18: Estimated vs. Actual Furnace Gas Temperature (MOP)

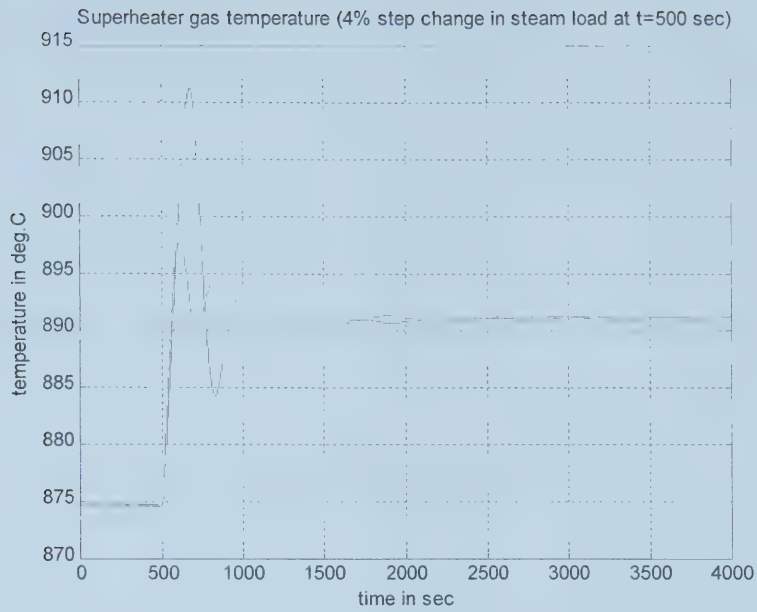


Figure 4.19: Estimated vs. Actual Super-heater Gas Temperature (MOP)

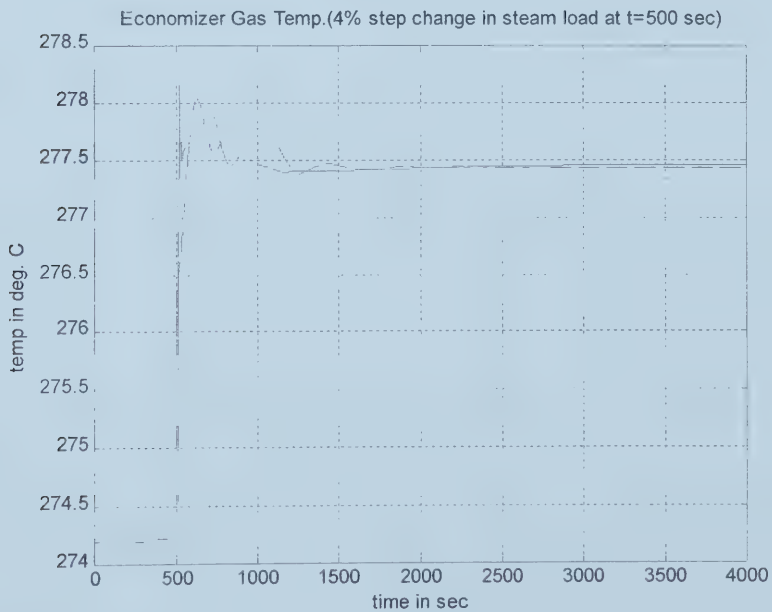


Figure 4.20: Estimated vs. Actual Economizer Gas Temperature (MOP)

4.4.3 Observer Design for LOP

The design procedure for Low Operating Point (LOP) is similar to the above two designs. The model for LOP has one real and a pair of complex poles. The pair of complex poles lies at $s = -0.0069 \pm 0.0176j$. Out of three zeros in total, one zero lies at $s = +0.0053$ which is right half plane zero. Therefore our choice for weight function \mathbf{W}_1 is:

$$\mathbf{W}_1 = 0.01 \left[\frac{(s + 0.0069 - 0.0176j)(s + 0.0069 + 0.0176j)}{s(s + 0.0053)} \right]$$

Singular values of the shaped plant \mathbf{P}_s are shown in figure 4.21. A sixth order Controller $\mathbf{G3}$ is obtained. The singular value plot of a sensitivity function, using controller $\mathbf{G3}$, is shown in figure 4.22 while output step response is given in figure 4.23. $\mathbf{G3}$ being high order controller is reduced by using Hankel norm approximation technique to a second order controller $\mathbf{G3}_h$. The singular value plot comparison of sensitivity function for original controller $\mathbf{G3}$ and reduced order controller $\mathbf{G3}_h$ is given in figure 4.24.

It can be observed from these results that the performance given by $\mathbf{G3}_h$ is the same as $\mathbf{G3}$. $\mathbf{G3}_h$ being a low order controller is selected as controller $\mathbf{G}(s)$ for our “Observer 3” (see figure 2.3). “Observer 3” is the observer designed for Low Operating Point.

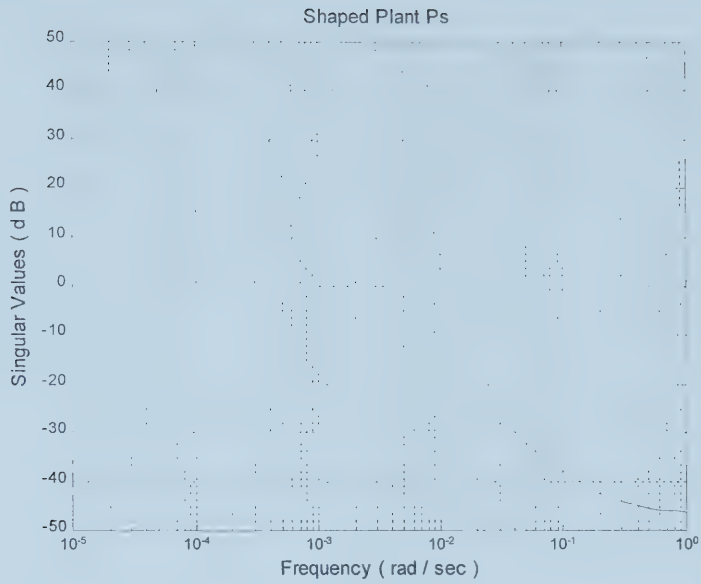


Figure 4.21: Shaped Plant P_s (LOP)

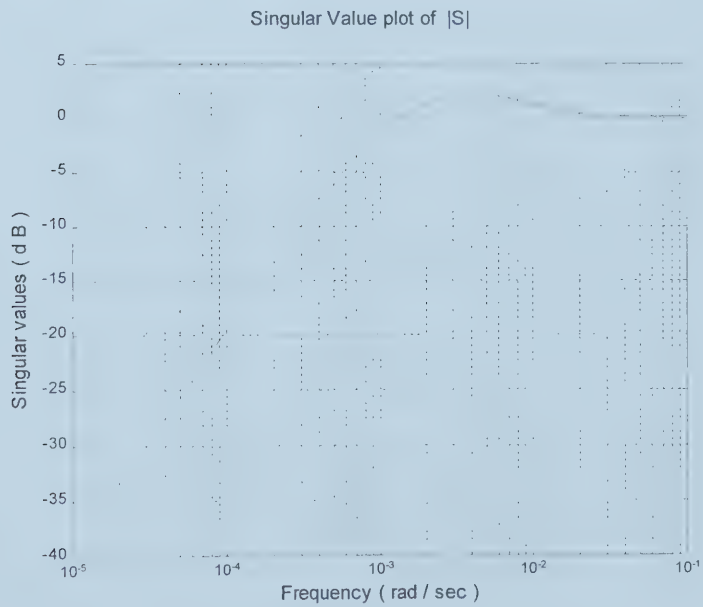


Figure 4.22: Singular value plot for $|S|$ using controller G_3 (LOP)

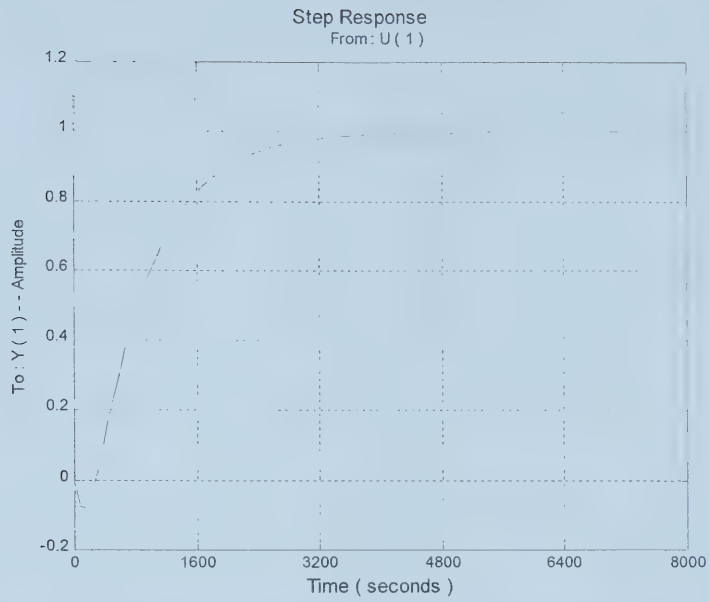


Figure 4.23: Output Step Response using controller G3 (LOP)

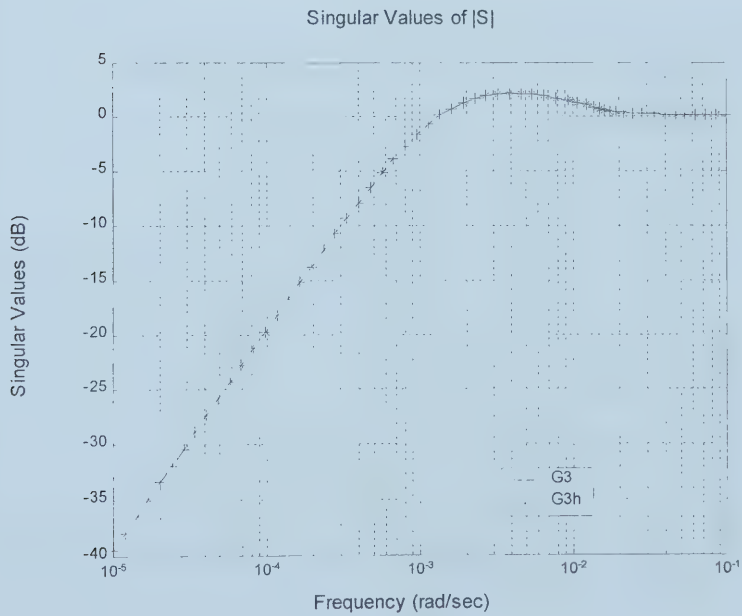


Figure 4.24: Singular value plot for $|S|$ with controller G3 and $G3_h$

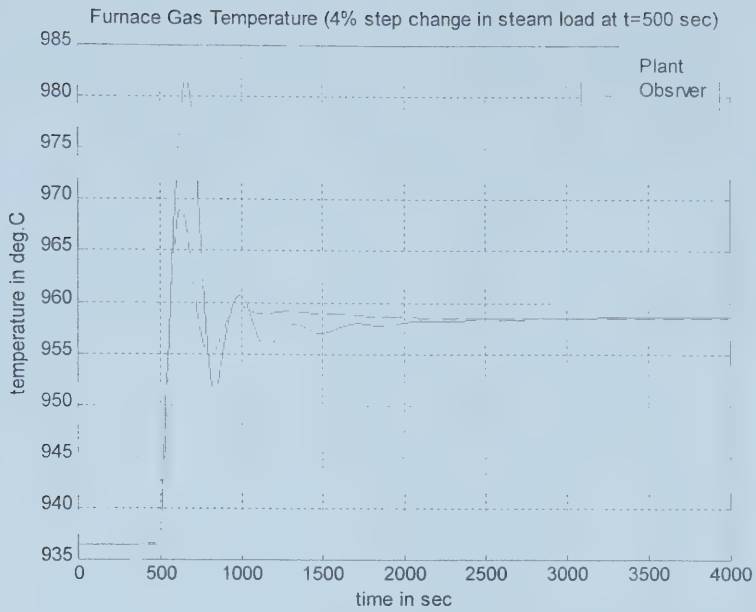


Figure 4.25: Estimated vs. Actual Furnace Gas Temperature (LOP)

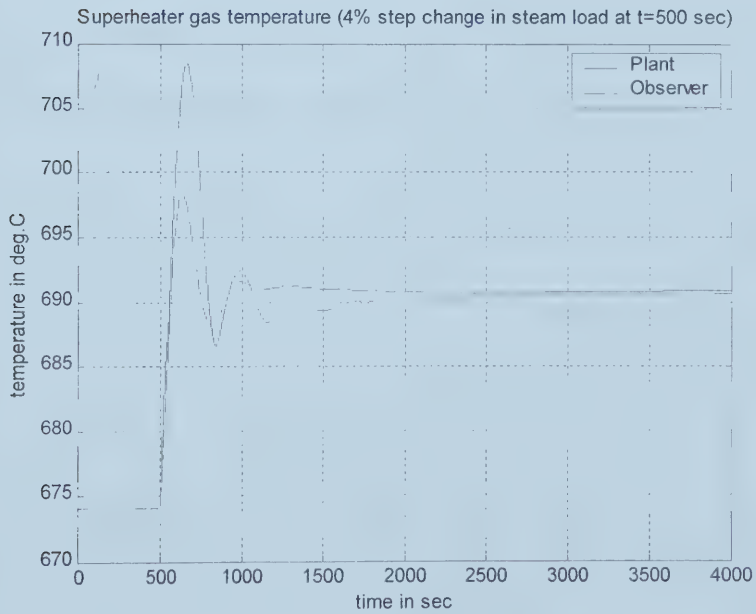


Figure 4.26: Estimated vs. Actual Super-heater Gas Temperature (LOP)

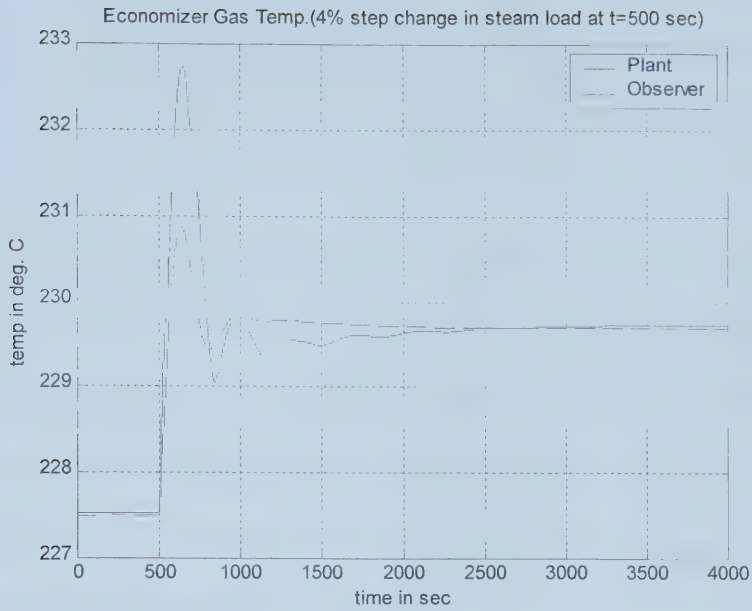


Figure 4.27: Estimated vs. Actual Economizer Gas Temperature (LOP)

A 4% change is applied at $t = 500$ seconds to SYNSIM boiler model and “Observer 3” simultaneously. Steam load is changed from steady state value of 117.2 kg/sec to 121.89 kg/sec. States estimated by the observer are compared with the actual states given by SYNSIM model. The comparison is given in figure 4.25, figure 4.26 and figure 4.27. The behavior of actual states at low operating point i.e. at low steam load, exhibits some non-linearity. It is almost impossible for a linear observer to exactly replicate the non-linear dynamics. But it can provide the closest possible linear approximation of the non-linear dynamics. Figure 2.25 to figure 2.27 shows that our observer is doing well by keeping the error between estimated state and actual state to zero as $t \rightarrow \infty$.

4.4.4 Comments:

For better performance in the presence of uncertainty, noise and disturbance, the following would be helpful.

Uncertainty effect

Controller **G** in the observer block should have good tracking properties so that it can follow any change in the plant output **y** efficiently. Moreover due to the Δ term in the plant, **y** will be different from \hat{y} . \hat{y} will follow **y** in the presence of uncertainty only if **G** has good tracking properties. This is the reason why we introduce integral action in our control loop by choosing suitable weight function **W₁**.

Disturbance & Noise rejection

Disturbance on plant input 'u', which could be any disturbance in low frequency, and similarly high frequency noise will affect the actual states of the plant. Therefore we want disturbance and noise on 'u' to be fed to the observer with out any attenuation so that the observer states can react the same way as the plant states.

Disturbance and noise on the output 'y' cannot be rejected and will directly appear in the error input to controller 'G'. It is a major limitation associated with this design method. Therefore it is recommended to choose such a plant output that has negligible low frequency disturbance on it or the effect of disturbance is insignificant. In the selection of output for boiler we have chosen drum pressure instead of drum level. Drum pressure has no disturbance acting on it. The drum level has low frequency noise component due to shrink and swell effect which acts as disturbance on actual drum level measurement.

Chapter 5

Observer Scheduling

This chapter deals with the problem encountered due to non-linearity of the process. A simple solution to the problem is provided through the concept of observer scheduling. The concept of observer scheduling is taken from the popular theory of Gain Scheduling. An observer bank is introduced to replace the single observer in order to cover the whole operating range. At any operating point, the states estimated by that observer are chosen which gives better performance around that point. The performance of the observer bank through the entire operating range of the boiler is shown in the form of simulation results.

5.1 Gain Scheduling

Physical systems have the inherent property of being non-linear. Good mathematical models of the real systems almost contain non-linear functions. Despite this fact, control system is often designed by using the simplified and linearized version of the original complex non-linear system. But linearized models are only good with in certain range around the normal operating point. In many cases, such as boilers that operate in a large operating range, the controllers designed using linearized models give poor performance at the operating points that are out of the region for normal operation.

One way to improve controller performance, while still employing linear techniques is to linearize the original non-linear plant at a number of different operating points, and then design linear controllers for each of the linearized models of the plant. As the plant condition changes the controllers can then be switched to give better performance all the time through the whole operating range. This technique is called “Gain Scheduling”.

This technique has been used successfully in many applications, particularly in those applications where there exists a measurable parameter that correlates well with the changes in the process. The concept of gain scheduling first came up during the development of flight control system. In this application, the controller parameters are adjusted based on the measurement of speed and dynamic pressure. Since the controller parameters must be calculated for various operating points and performance must be checked by extensive simulation, there is a big computational burden involved in the design. However due to the advancement in high-speed hardware, which has increased the computational power of microprocessors, makes it possible to easily implement gain scheduling. The controller parameters can be changed very quickly in response to changing operating conditions. That is the reason why gain scheduling has become a widely used design methodology for many non-linear practical systems.

An elementary introduction to gain scheduling along with the idea of its application is given by K. J. Astrom and B. Wittenmark [29]. W. J. Rugh [30] has discussed the analytical framework for the design of gain-scheduled controller for non-linear systems. He has given some suggestions to deal with difficulties during the design

process. J. S. Shamma and M. Athens [31] & [32], have provided a set of theorems to ensure the stability, performance and robustness of the gain scheduled controller. But these have little significance, because of the difficulty to obtain information requirements of these theorems. Recently H. J. Marquez [29] has applied Gain scheduling theory to systems described by multiple models.

5.2 Observer Scheduling

Observer scheduling is not a new concept but a modification of the existing gain scheduling theory. For a nonlinear system, models are identified at a number of different operating points. Observers are designed for each model. These observers are connected to the plant to form an observer bank. A switching mechanism is provided to select the particular observer as a source of estimated state values. This switching operation is based on the measured values of a parameter, which has strong correlation with internal conditions of the process. The value of that parameter within or out of certain specific range is called scheduling criteria. The regions of operation of the adjacent observers are overlapped so as avoid any poor performance around the switching point. A dead band in the switching logic is important around the switching point. This is to avoid chattering operation between two adjacent observers when the process varies above and below the switching point within certain predefined range. The idea of observer scheduling is simple and is an efficient tool to tackle non-linear systems.

Observer design, in our case, is basically a controller design problem. Therefore observer scheduling design problem is in fact a gain scheduling design problem. We

can directly apply the gain scheduling theory and subsequently all the benefits and drawbacks associated with the Gain scheduling would be the benefits and drawbacks of the observer scheduling. Without going into much detail on theoretical side, we would rather focus on the practical application of this concept and would draw conclusions from the simulation results for boiler state estimation application. At a later stage, the possibility of replacement of “Multi-observer Bank” by “SYNSIM Model based Gain scheduled Observer” would be discussed for practical application of the whole concept.

5.3 Simulation Results

From previous chapters, it is known that the whole operating range of the utility boiler is divided into three segments. Operating point at the middle of each segment is selected to identify model for that operating region. The three models identified are differentiated as High Operating Point (HOP) model, Middle Operating Point (MOP) model and Low Operating Point (LOP) model. Our proposed observer has two components. The model and the compensator/controller $\mathbf{G}(s)$ (see figure 2.3). The controller associated with HOP is denoted by $\mathbf{G1}$, with MOP by $\mathbf{G2}$ and with LOP by $\mathbf{G3}$. Observer1 consists of $\mathbf{G1}$ and model HOP, Observer2 consists of $\mathbf{G2}$ and model MOP and Observer3 consists of $\mathbf{G3}$ and model LOP. In each observer the controller and model are connected to each other and to the plant as shown in figure 2.3. All the three observers are connected to a switching mechanism collectively called Observer Bank, as shown in figure 5.1.

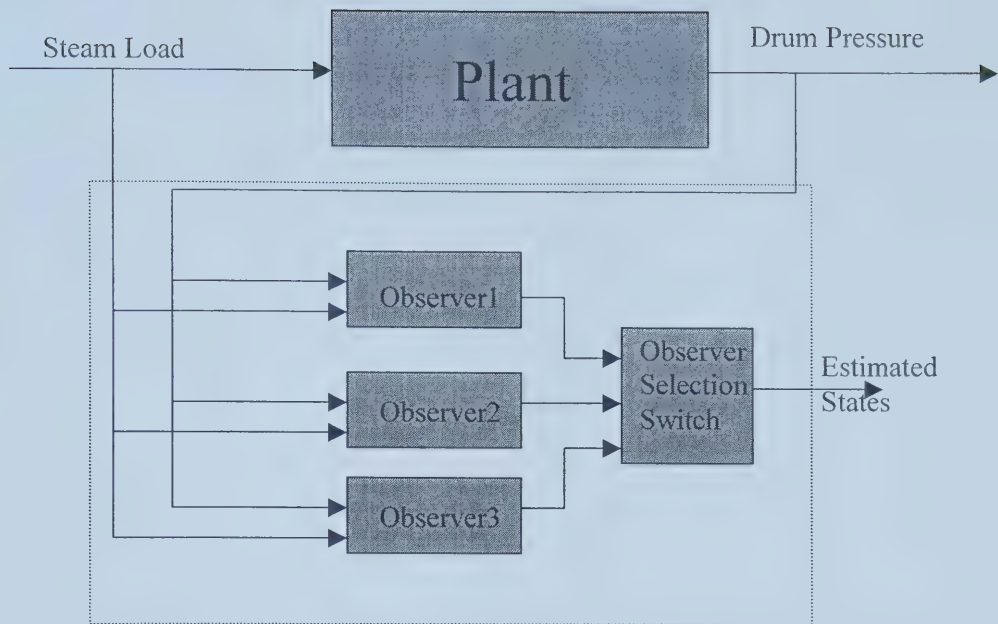


Figure 5.1 Observer Scheduling Implementation Layout

Inputs to the Observer Bank are plant input (steam load) and plant output (drum pressure) while the output is the estimated vector of the plant states. Steam load is selected as a switching parameter, mainly due to its high degree influence on the plant states. As mentioned earlier, throughout our simulation Simulink based dynamic model SYNSIM is used as a plant.

Switching mechanism is designed by using logic blocks provided in the Simulink library. After comparing the individual observer behavior with the plant dynamics for the whole operating window, points to switch the observers are selected. The upper and lower limits of the overall operating region are steam load of 116 kg/sec.

to 260 kg/sec. respectively. Steam load of 150 kg/sec and 230 kg/sec are selected as switching points. Steam load is changed as shown in figure 5.2. The net change consists of eight steps. The first step represents a change of 4 kg/sec while all other steps represent changes of 20 kg/sec each.

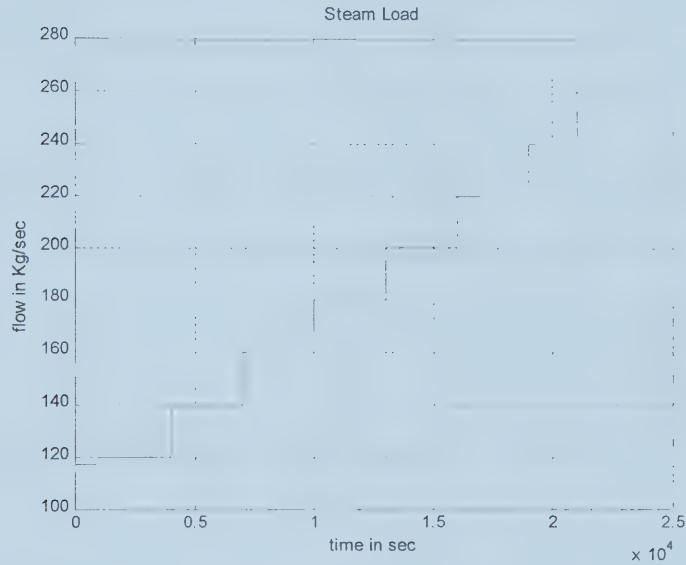


Figure 5.2: Multi-Step Steam Load Change

Simulation time of 25000 seconds is selected so as to give enough time to the process to settle down after each step. The size of each step is chosen such that each step is comparable to the maximum practically possible step change. In practice the operators ensure that the plant change its state slowly and in small steps. Large and sudden changes are fatal to the plant stability and are usually avoided.

Figure 5.3 shows the relationship between “Estimated Furnace Gas Temperature”, estimated by Observer1 (observer designed for HOP), and the “Actual Furnace Gas Temperature”. It can be observed that the performance of “Observer1” is acceptable with in the region where steam load is high. There is a large error between actual and estimated state with in low and medium steam load regions. This error could eventually be reduced provided the system was kept in steady state for a long time, which practically is not possible.

Figure 5.4 shows the relationship between “Estimated Furnace Gas Temperature”, estimated by Observer2 (observer designed for MOP), and the “Actual Furnace Gas Temperature”. It can be observed that the performance of “Observer2” is acceptable with in medium steam load region. The error between actual and estimated state with in low and high steam load regions is very large.

Figure 5.5 shows the relationship between “Estimated Furnace Gas Temperature”, estimated by Observer3 (observer designed for LOP), and the “Actual Furnace Gas Temperature”. It can be observed that the performance of “Observer3” is acceptable with in high steam load region. The error between actual and estimated state with in low and medium steam load regions is extremely large which is not desirable. Specifically at the high end, the estimated value is 1900 degree Celsius while the actual furnace gas temperature is 1300 degrees.

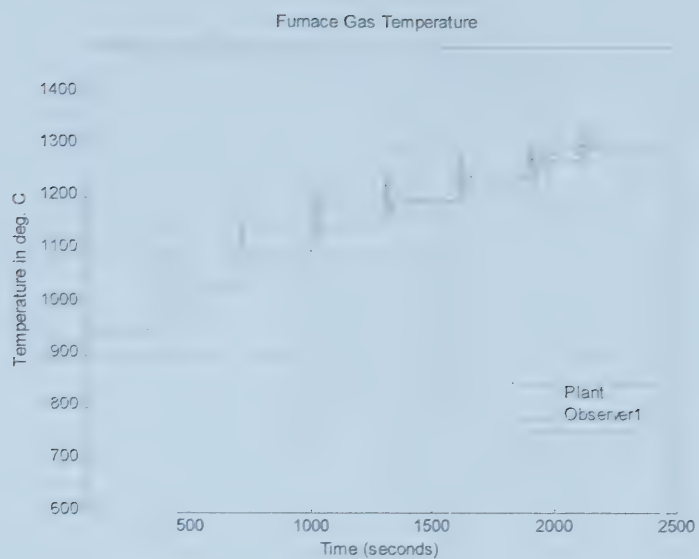


Figure 5.3: Furnace Gas Temperature (Plant vs. Observer1)

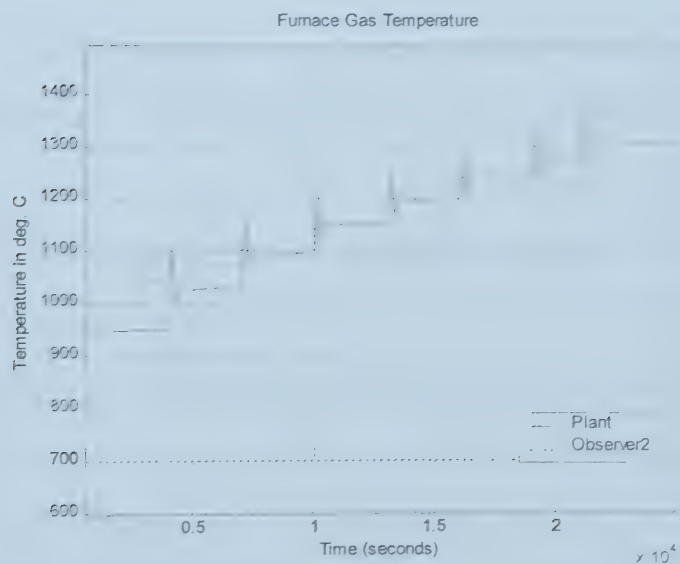


Figure 5.4: Furnace Gas Temperature (Plant vs. Observer2)

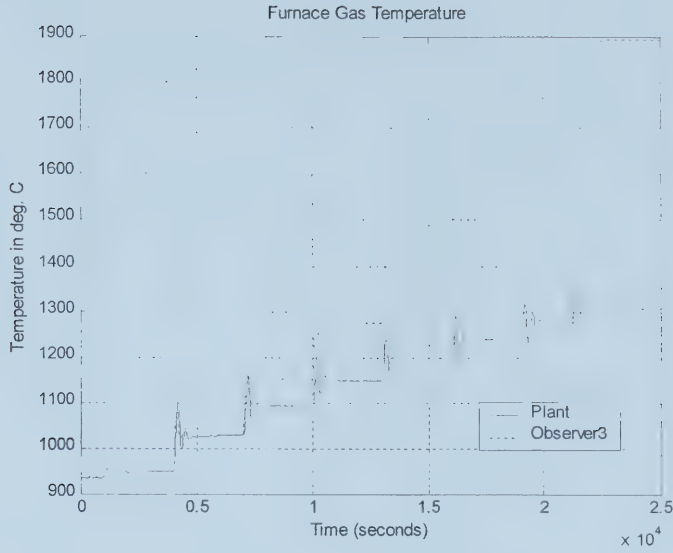


Figure 5.5: Furnace Gas Temperature (Plant vs. Observer3)

Figure 5.6 to 5.8 shows the comparison between “Actual Super Heater Gas Temperature” and “ Estimated Super Heater Gas Temperature” for all the three observers. Similarly, Figure 5.9 to 5.11 shows the comparison between “Actual Economizer Gas Temperature” and “Estimated Economizer Gas Temperature”. The conclusion in these two cases is the same as drawn from the figures 5.3 to 5.5.

It is clear from these results that Observer1 performs well in the high steam load region, Observer2 in the medium steam load region and Observer3 in the low steam load region. This brings us to a conclusion that the observer is performing well in the region for which it is design while it has extremely poor performance outside its designed operating region.

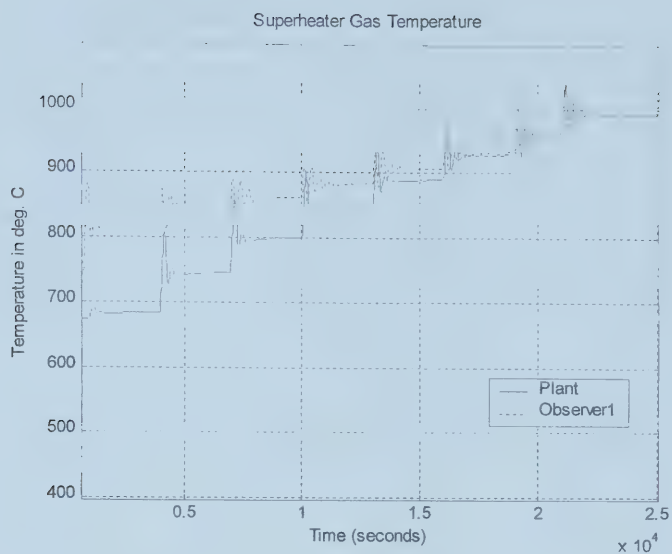


Figure 5.6: Super Heater Gas Temperature (Plant vs. Observer1)

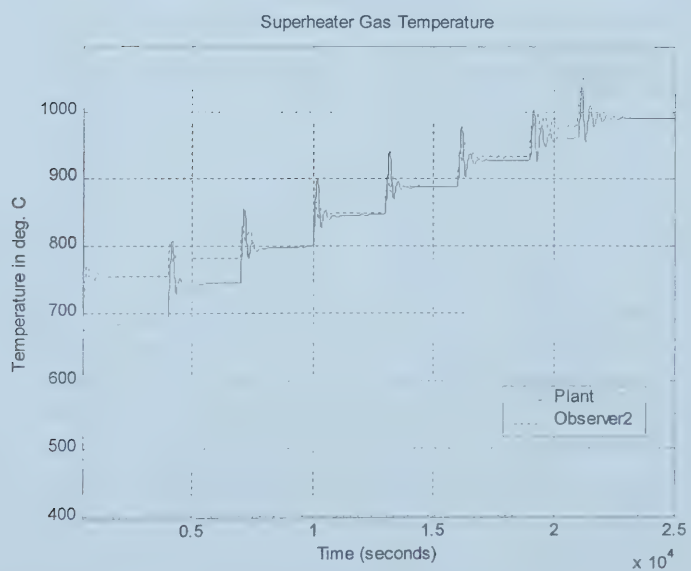


Figure 5.7: Super Heater Gas Temperature (Plant vs. Observer2)

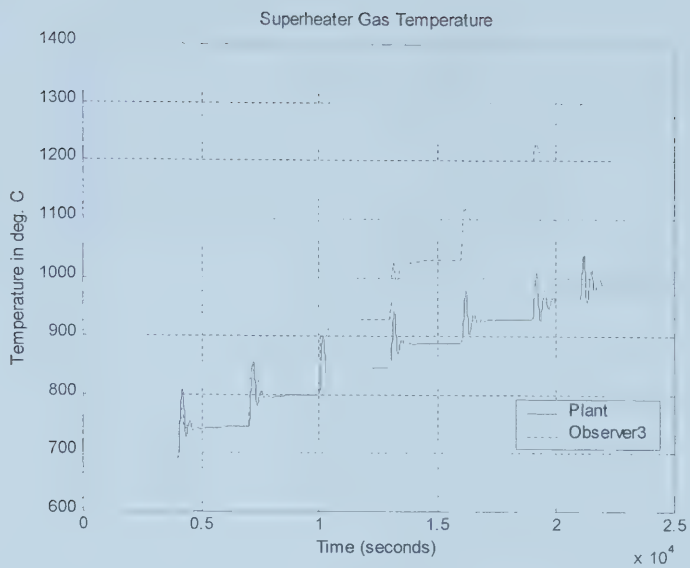


Figure 5.8: Super Heater Gas Temperature (Plant vs. Observer3)

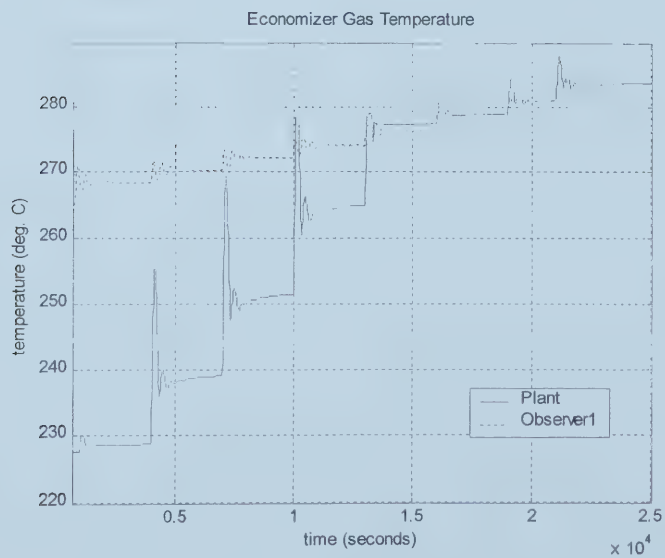


Figure 5.9: Economizer Gas Temperature (Plant vs. Observer1)

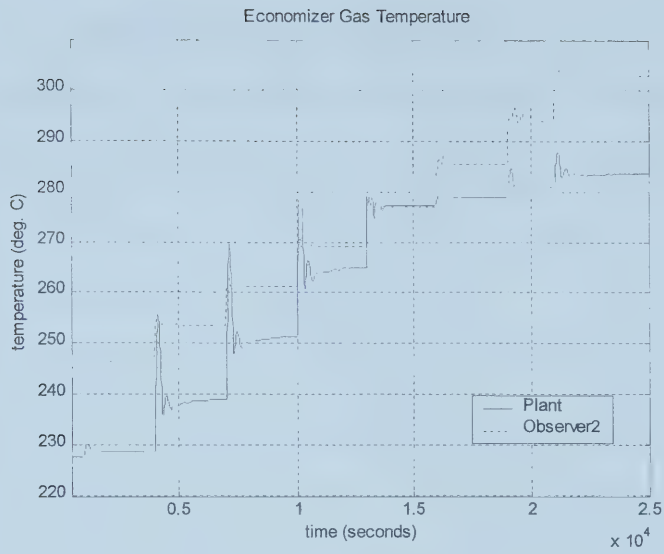


Figure 5.10: Economizer Gas Temperature (Plant vs. Observer2)

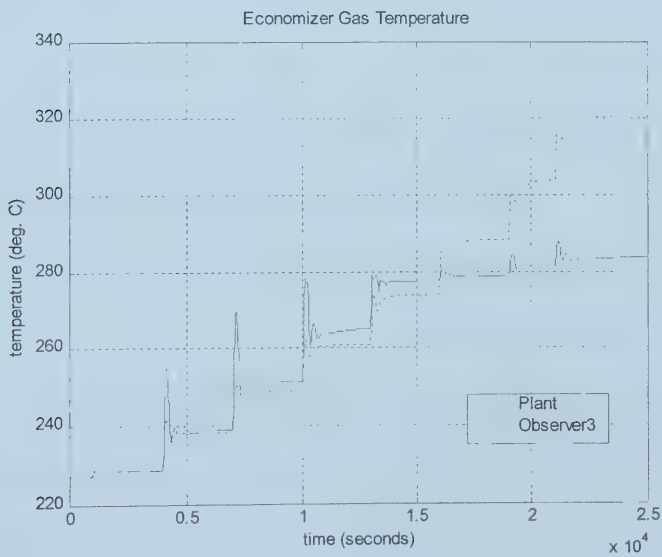


Figure 5.11: Economizer Gas Temperature (Plant vs. Observer3)

To verify that observer scheduling is working well, the output of the Observer Bank (estimated state vector) is compared with the actual plant state vector. Observer Bank consists of three observers and a switching mechanism that is used to select the estimated parameters of that observer which provides best estimation out of the three. Figure 5.12 to 5.14 shows the comparison between estimated states (estimated by the observer Bank) and the actual states. Observer switching is performed at the steam loads of 150 kg/sec and 230 kg/sec.

It can be observed that the estimated state follows almost the same trajectory as the actual state. Except for the economizer gas temperature which deviates from the actual at the medium steam load. This is probably because of highly non-linear nature of the energy exchange mechanism between boiler feed water and the exhaust gas. This comparatively more non-linearity in the economizer gas temperature can be tackled by dividing the whole operating range into more segments. Right now the whole operating range is divided into three segments and hence three models are identified. By increasing the number of selected operating points and the subsequently increasing the number of observers would improve the performance and the problem like one in figure 5.14 can be eliminated.

From the process knowledge and after several simulation runs it is concluded that six observers would be sufficient to give optimum results while implementing it practically. That would require six different models at six different operating points. But for the purpose of study we keep our selves restricted to three models to keep the problem simple.

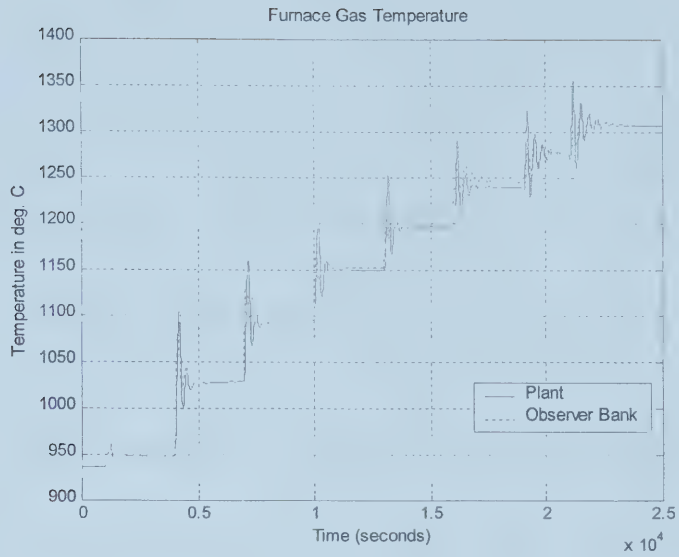


Figure 5.12: Furnace Gas Temperature (Plant vs. Observer Bank)

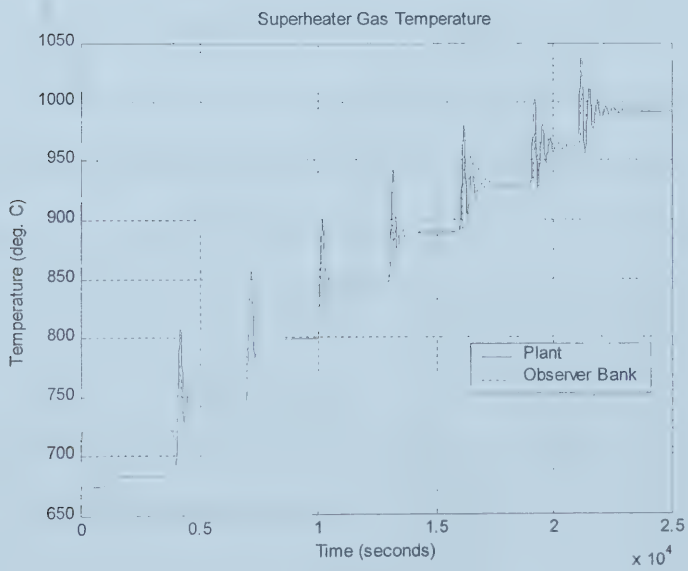


Figure 5.13: Super Heater Gas Temperature (Plant vs. Observer Bank)

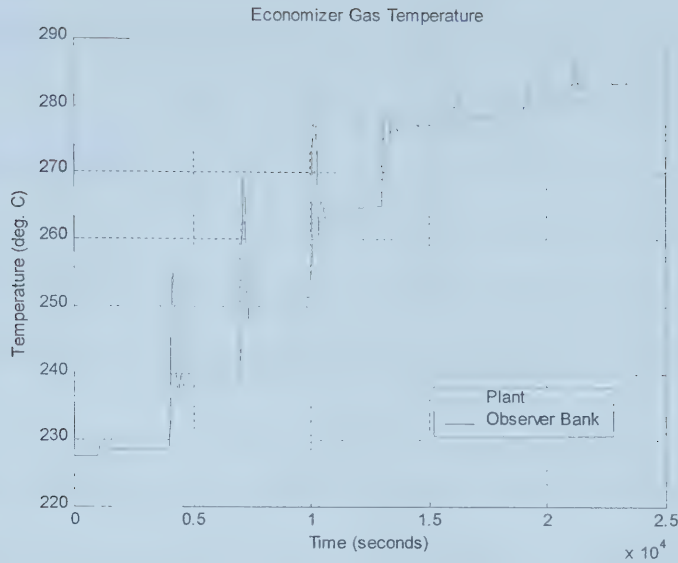


Figure 5.14: Economizer Gas Temperature (Plant vs. Observer Bank)

At practical implementation stage on the real plant, the input and output signals would be taken from the transmitters installed for measurement and SYNSIM dynamic model would need modification for real time processing. The real time non-linear SYNSIM model would be used as a part of the Observer instead of state space model. Six controllers would be designed using six linear state space models. These controllers would be used in a manner that -only that controller $G(S)$ would be connected to SYNSIM, which is designed for that operating segment. This would transform the Observer scheduling problem into simple Gain Scheduling problem. The estimated states from the SYNSIM would be the required states corrected by the signal from the selected controller. This would reduce the work to design observers and would increase accuracy of the state estimator.

Chapter 6

Conclusion

In this chapter, the conclusion drawn in each of the previous chapters is summarized with the critical look at the advantages and disadvantages of the proposed method.

A dynamic state estimator for systems with plant-model mismatch and unknown disturbance and noise is investigated and the design and analysis of input-output observer is carried out. The linear observer design theory is extended to tackle non-linearity in real systems. The following is the summary of our conclusion:

1. According to our approach, observer design becomes H_∞ controller design. This enables the designer to fully utilize the vast literature related to this theory. It also provides flexibility to designer to choose any method out of several available methods.
2. This method provides better insight if one is interested in the frequency characteristics of the observer. From beginning to end, the design process is transparent. The performance limitations such as right half zeros can be seen at the early stage of the design. In other observers it can only be seen at later stages.

3. Fault detection problem can be posed as estimation problem and consequently as an equivalent control problem. This refers to fault detection algorithms based on observer banks.
4. Observer scheduling works well for non-linear systems provided the whole operating range is divided into suitable number of segments such that the system behavior is linear within each segment. Selection of individual observer should be based on a parameter that plays dominant role in changing the state parameters. Controller is an integral part of input-output observer and hence the “Observer Scheduling” problem reduces to “Gain Scheduling” problem.
5. Although the observer design becomes feedback design, the objectives are still different. In case of typical control problem we avoid the overshoot of sensitivity function from zero dB and allow for smooth transition of the function from negative value to zero value without a significant bump on the positive side. In case of observer to get the required speed of response, slight overshoot from the zero dB in high frequency region is acceptable without losing much on the performance side.

In short there is always a compromise between the speed of response, low error due to uncertainty, robustness against disturbance and noise.

6. Output error sensitivity function is minimized instead of state error sensitivity function \mathbf{H} in eq.(2.25). \mathbf{H} is solvable if and only if matrix $\mathbf{F}_0\mathbf{G}$ is a square matrix i.e. the dimension of the output is at least equal to the number of states. This is similar to flat plant control problem. In case of flat plant sensitivity minimization control problem, a clean solution to the problem is available only in the case where the plant has at least as many inputs as outputs [34].

Therefore it is concluded that in case of observer it is not possible to minimize a state error due to uncertainty unless we have the same number of measured variables as that of the states. This is an important result which has been discovered during the study.

7. The order of the controller part of the observer obtained as result of this design is usually very high. The order of the H_∞ controller is always equal to or greater than the order of the plant model. However controller order reduction techniques such as Residualization and Hankel norm approximation, some time, works well with out compromise on the performance.

A multivariable PID approximation [35] can be obtained by truncating the Maclaurin expansion of the controller with respect to the variable ' s '. This approximation is only true with in the low frequency range and may not be realizable in some cases.

8. Selection of suitable weighting functions is a tricky task and is time consuming.
A fair amount of process knowledge is required to come up with good weighting functions.
9. Luenberger observer is good in the speed of response and could be a better choice if frequency characteristic is not an issue.

Bibliography

- [1] K. Gooden, Peter Morgan & David White, “*NSERC project Proposal*”, Syncrude Canada Ltd. Alberta.
- [2] Raymond Rink et al, “*Synsim Document*”, Syncrude Canada Ltd. Alberta.
- [3] K.J. Astrom, R.D. Bell, “*Drum Boiler Dynamics*”, *Automatica*, vol. 36, pp. 363-378, 2000.
- [4] P. M. Derusso, ...[et al], “*State variables for Engineers*”, 2nd edition, John Wiley & Sons, Inc. NewYork, 1998, pg.366.
- [5] H. J. Marquez, “*An input-output approach to state estimation*”, submitted for publication.
- [6] C.T. Chen, “*Linear system theory and design*”, Holt, Rinehart and Wiston, 1984.
- [7] M. Verma and E. Jonchheere, “ *\mathcal{L}_x compensation with mixed sensitivity and a broad band matching problem*”, *Systems and Control Letters*, vol. 4, pp. 125-129, 1984.
- [8] Peter Van Overschee and Bart De Moor, “*N4SID: Subspace algorithms for the identification of combined deterministic-stochastic systems*”, *Automatica*, vol. 30, No. 1, pp. 75-93, 1994.
- [9] D. E. Rivera and S.V. Gaikwad, “*Systematic techniques for determining modeling requirements for SISO and MIMO feedback control*”, *Journal of Process Control*, vol. 5, pp. 213-224, 1995.
- [10] Jong-Koo Park, “*The concept and design of dynamic state estimation*”, proc. of Amer. Cont. conference, San Diego, California, June 1999.
- [11] S. Skogestad and Ian Postlethwaite, “*Multivariable Feed Back Control-Analysis and Design*”, John Wiley & Sons, New York, Jan. 1997.
- [12] D. Luenberger, “*Observers for multivariable systems*”, *IEEE Trans. On Automatic control*, vol.11, pp.190-197, 1996.
- [13] R.E. Kalman, “*A new approach to linear filtering and prediction problems*”, *ASME J. of Basic Engg., Serv. D*, vol. 82, pp. 34–45, 1960.
- [14] R.E. Kalman and R. S. Bucy, “*New results in linear filtering and prediction theory*”, *ASME J. of Basic Engg., Serv. D*, vol. 83, pp. 95–108, 1961.
- [15] L. Xie and Y. C. Soh, “*Robust Kalman filtering for uncertain systems*”, *Systems and Control Letters*, vol. 22(2), pp. 123-129, 1994.
- [16] Bernstien and W. Haddad, “*Steady state Kalman filtering with an H_∞ error bound*”, *Systems and Control Letters*, vol. 12, pp 9-16, 1987.
- [17] I. R. Peterson and D.C. McFarlene, “*Robust state estimation for uncertain systems*”, proc. of 30th IEEE conf. on Decision & Control, Brighton, England, 1991.
- [18] R. Nikoukhah, S. L. Campbell, and F. Delebecque, “*Observer design for general linear time-invariant systems*”, *Automatica*, vol.34, no. 5, pp. 575-583, 1998.

- [19] A. S. Willsky, "*A survey of design methods for failure detection in dynamic systems*", Automatica, vol. 12, pp. 601-611, 1976.
- [20] R. J. Patton and J. Chen, "*Robust fault detection and isolation (FDI) systems*", Control and Dynamic Systems, vol. 74, pp.171-224, 1996.
- [21] G. Zames, "*Feedback and optimal sensitivity: model reference transformation, multiplicative seminorms, and approximate inverse*", IEEE trans. on automatic ctrl. , vol. 26, pp. 301-320, 1981.
- [22] K. Glover and J. C. Doyle, "*State space formulae for all stabilizing controllers that satisfy an H_∞ norm bound and relations to risk sensitivity*", Systems and control letters, vol. 11, pp. 167-172, 1988.
- [23] J. C. Doyle, K. Glover, P. P. Khargonekar and B. A. Francis, "*State space solution to standard H_2 and H_∞ control problems*", IEEE trans. on automatic ctrl. vol. 34(8), pp. 831-847, 1989.
- [24] M. G. Safanov, D. J. N. Limebeer and R. Y. Chiang, "*Simplifying the H_∞ theory via loop shifting, matrix-pencil and descriptor concepts*", International journal of control, vol. 50(6), pp. 2467-2488, 1989.
- [25] M. Green and D. J. N. Limebeer, "*Linear robust control*", Prentice-Hall, Englewood Cliffs, 1995.
- [26] D. Mcfarlane and K. Glover, "*Robust controller design using normalized co-prime factor plant description*", Lecture notes in Ctrl. & Information Sciences, vol. 138, Springer-Verlag, Berlin, 1990.
- [27] R. A. Hyde, "*The application of robust control to VSTOL aircraft*", PhD. thesis, University of Cambridge, 1991.
- [28] K. Glover and D. Mcfarlane, "*Robust stabilization of normalized co-prime factor plant description with H_∞ bounded uncertainty*", IEEE trans. on automatic ctrl., vol. 34(8), pp. 821-830, 1989.
- [29] K. J. Astrom and B. Wittenmark, "*Adaptive Control (second edition)*", Addison-Wesley publishing Co., 1995.
- [30] W. J. Rugh, "*Analytical framework for gain scheduling*", IEEE control system magazine., vol. 11, pp. 79-84, 1991.
- [31] J. S. Shamma and M. Athens, "*Analysis of nonlinear gain scheduled control systems*", IEEE trans. on Automatic control, vol. AC-35, pp. 898-907, 1990.
- [32] J. S. Shamma and M. Athens, "*Gain scheduling: Potential hazards and possible remedies*", IEEE control system magazine, vol. 12, pp. 101-107, 1993.
- [33] H. J. Marquez, "*An input-output approach to systems described using multiple models*", IEEE trans. on circuits and systems, Part-I: Fundamental theory and applications, 1999.
- [34] M. Vidyasagar, "*Control System Synthesis: A factorization Approach*", The MIT press, London, England, 1987, pp. 188.
- [35] W. Tan, Y. G. Niu, and J. Z. Liu, "*H-infinity control for a boiler-turbine unit*", Proc. IEEE Conference on Control Applications, Hawaii, USA , 1999.

Appendix A

Parameter	Units	Low Operating Point	Middle Operating Point	High Operating Point
Fuel flow	Kg/sec	1.509	2.879	3.936
Air Flow	Kg/sec	27.94	53.3	72.87
Spray flow	Kg/sec	0	0	0.9961
Furnace Gas Temperature	°C	936.1	1181	1291
Super Heater Gas Temperature	°C	674.1	874.7	975.8
Drum Pressure	KPa	6368	6566	6769
Steam Temperature	°C	439.6	490	500

Table A1: Steady State Process Parameter for Selected Operating Points

Appendix B

Controller $G1_c$

A1_c =

0	0.3984	1.6061	-26.7970
0	0.9793	3.9380	-66.3480
0	-0.0344	-0.1441	2.34180
0	0.0128	0.0512	-0.86658

B1_c =

0.049143
0.062732
-0.001202
0.000904

C1_c =

0.032 0 0 0

D1_c =

0

Eigenvalues of **G1_c**:

0
-0.0121 + 0.0276i
-0.0121 - 0.0276i
-0.0072

Eigenvalues of closed loop system $(P^*G1_c)/(1+P^*G1_c)$

-0.0024 + 0.0193i
-0.0024 - 0.0193i
-0.0074
0
-0.0121 + 0.0276i
-0.0121 - 0.0276i
-0.0072
-0.0084 + 0.0224i
-0.0084 - 0.0224i
-0.0042 + 0.0198i
-0.0042 - 0.0198i
-0.0036
-0.0073
-0.0075

Controller G1

A1 =

-0.01260	0	-0.03577	-0.18439	0.02779	-1.1955
0.03125	0	0	0	0	0
0	0	0.17339	0.86308	-0.16154	5.8070
0	0	0.23645	1.20590	-0.18355	7.9011
0	0	-0.01522	-0.09287	-0.00362	-0.5622
0	0	-0.04363	-0.22197	0.03522	-1.4584

B1 =

0.07521
0
-0.52998
-0.49844
-0.00132
0.09635

C1 =

-0.02496	0.04096	-0.11449	-0.59003	0.088929	-3.8254
----------	---------	----------	----------	----------	---------

D1 =

0.24068

Controller G1r

A1_r =

-0.070023	-0.005222	0.00840	0
-0.005222	-0.006805	0.02245	0
-0.008406	-0.022435	-0.44708	0
0	0	0	1.6e-018

B1_r =

0.13069
0.0049454
0.0078401
-0.0033526

C1_r =

-0.13069 -0.0049454 0.0078401 -0.39538

D1_r =

0.24056

Controller G1h

A1_h =

0.0001953 -0.004298
0.0030622 -0.067379

B1_h =

-0.03513
0.12661

C1_h =

-0.024861 -0.12576

D1_h =

0.23795

Controller G2

A2=

-0.0091	0	-0.015429	-0.08642	0.00688	-0.13603
0.0312	0	0	0	0	0
0	0	0.106200	0.58124	-0.04958	0.96197
0	0	0.091001	0.49928	-0.03937	0.80125
0	0	-0.011720	-0.06951	-0.00214	-0.10226
0	0	-0.075459	-0.41728	0.03453	-0.67109

B2 =

0.078109
0
-0.75063
-0.46274
0.005254
0.40503

C2 =

0.00032 0.03072 -0.049371 -0.27656 0.022021 -0.4353

D2 =

0.24995

Controller G2_h

A2_h =

0.0002028 -0.003962
0.0028576 -0.055825

B2_h =

0.036649
-0.11216

C2_h =

0.026272 0.11149

D2_h =

0.25182

Controller G3

A3 =

-0.0053	0	0.008372	-0.11260	0.008263	-0.13096
0.01562	0	0	0	0	0
0	0	0.034049	-0.46668	0.034342	-0.56089
0	0	-0.017472	0.22646	-0.016689	0.27036
0	0	0.013041	-0.15728	0.005671	-0.18365
0	0	0.018183	-0.24847	0.018589	-0.29366

B3 =

0.022446
0
0.14114
-0.047925
0.0010151
0.051156

C3 =

0.00544 0.016384 0.0053583 -0.072064 0.005288 -0.083813

D3 =

0.014366

Controller G3h

A3h =

1.9596e-005 -0.00058112
0.000405850 -0.01203600

B3h =

-0.026459
0.02197

C3h =

-0.018476 -0.021965

D3h =

0.015236

University of Alberta Library



0 1620 1515 7900

B45615